Title

Phylo-Plex: A phylogenetically informed, low-cost amplicon sequencing platform for deployable high-resolution genomic epidemiology

Authors

Mathew A Beale[1,*], Vignesh Shetty[1], Kirsty E Ambridge[1], George Lacey[1], Sam Dougan[1], William Roberts-Sengier[1], Beth Sampher[1], Florent Lassalle[1], Matthew J Dorman[1,2], Mahlape P Mahlangu[3], Johanna ME Venter[3], Bianca Da Costa Dias[3], Martha Chipinduro[4,5], Tendai M. Washaya[4], Luanne Rodgers[4], Beauty Makamure[4], Ethel Dauya[4], Michael Marks[6,7,8], Etienne E. Müller[3], Rashida A Ferrand[4,6], Nicholas R Thomson[1,6]

[1]Parasites and Microbes Programme, Wellcome Sanger Institute, Cambridgeshire, UK
[2]School of Mathematical and Statistical Sciences, College of Science and Engineering, University of Galway, University Road, Galway, Ireland
[3]Centre for HIV & STIs, National Institute for Communicable Diseases, Johannesburg, South Africa
[4]Biomedical Research and Training Institute, Harare, Zimbabwe
[5]Faculty of Medicine and Health Sciences, Midlands State University, Gweru, Zimbabwe
[6]Faculty of Infectious and Tropical Diseases, London School of Hygiene and Tropical Medicine, London, UK
[7]Hospital for Tropical Diseases, University College London Hospital, London, UK
[8]Division of Infection and Immunity, University College London, London, UK

*Correspondence to mathew.beale@sanger.ac.uk

Abstract

Genomic pathogen surveillance is a powerful tool for public health and research, but is costly and unachievable in low-resource settings. Most sub-genomic typing methods sacrifice resolution whilst remaining costly. We developed “Phylo-Plex”, a novel approach that identifies information-rich genomic regions to maximise phylogenetic information whilst minimising the number of regions. Applied to *Treponema pallidum*, we designed a high-resolution multiplex PCR sequencing scheme for lineage tracking. Using MinION Flongle

cells, we sequenced 72 clinical samples. Our *T. pallidum* scheme comprising 59 multiplex amplicons achieved high discrimination of fine-scale sublineages comparable to those defined using whole genomes, and demonstrating a qPCR detection limit ≤Ct 32. Variant calls from MinION amplicon sequencing were highly correlated with Illumina whole genome sequencing. We successfully deployed the method in a low-resource laboratory in Zimbabwe, costed at <£300/24 samples (£12.47/sample). Phylo-Plex enables low-cost tracking of priority pathogenic lineages in low resource settings and at scale.

Introduction

Genomic pathogen surveillance has proven itself a powerful tool for both public health epidemiology and research[1]. Discriminating closely related isolates and deconvoluting complex samples and communities can enable finescale global tracking of pathogen populations, provide insights into epidemiology, transmission and the impact of clinical interventions such as antimicrobial usage or vaccines[2]. However, whole genome sequencing (WGS) pathogens at scale has substantial barriers to implementation including cost, complexity of data analysis, and time to results. This is particularly the case for low-resource settings or where pathogens cannot be readily cultured, necessitating direct or enriched metagenomic sequencing from clinical swabs and complex analytics[3,4]. Current alternatives to WGS, such as single gene or multi-locus sequence typing (MLST) are comparatively low resolution and are not responsive to the evolutionary dynamics of the target pathogen[5–8]. A solution to this is multiplex PCR[9–12] approaches such as the ARTIC network protocol (https://artic.network/)[11], which was used during the SARS-CoV-2 pandemic to generate over 18 million complete viral genome sequences. This allowed near real-time tracking of the virus and, because of the small size of the genome (30Kb), allowed for comprehensive identification of variants of interest and concern globally. However, this approach is not cost effective for generating larger complete bacterial genomes which range between 1-8 Mb in length, necessitating a more targeted approach.

Syphilis, caused by the bacterium *Treponema pallidum subspecies pallidum*, is an important sexually transmitted infection. Globally, *T. pallidum* causes 8 million new cases per annum and 700,000 cases of congenital syphilis leading to 220,000 early foetal deaths, stillbirths or neonatal deaths[13]. In most countries diagnosis of syphilis is restricted to either serological testing (in the context of antenatal care) or syndromic management (in the context of symptomatic individuals). *T. pallidum* is extremely difficult to culture[14] and so whole genome-based surveillance of syphilis is not widely used, even in high resource settings. Until now

the majority of available genomes have been sequenced with costly sequence capture enriched metagenomic approaches which require detailed bioinformatic analysis and significant computational infrastructure[8,15–17].

In this study, we developed and employed a novel approach for selecting optimal genome regions which can be targeted for multiplex PCR, dubbed “Phylo-Plex”. Given a representative collection of pathogen genomes, Phylo-Plex clusters single nucleotide polymorphisms (SNPs) along lineage-defining phylogenetic branches into information-rich amplicons which maximise resolution whilst minimising the number of genomic regions required for sequencing. This approach yields high-resolution phylogenies which recapitulate population structures obtained from WGS data, and can be performed quickly and easily at a fraction of the cost. Using *T. pallidum* as a model, we developed a high resolution Phylo-Plex scheme comprising 59 multiplex amplicons. We deployed our method in Harare, Zimbabwe and show how, when paired with low-cost nanopore sequencing, this approach provides a fast and flexible framework for SNP-based molecular sequence typing, that can be performed in a low resource setting at low cost. Phylo-Plex is universally applicable to any pathogen where we have existing genomic data and key lineages need to be found or priority pathogens need to be tracked.

Results

The Phylo-Plex approach we developed here takes WGS data from a representative global population framework, and identifies all discriminating SNPs linked to the major topological features (lineages, sublineages, etc) within the phylogeny. Then, regardless of the nature of any individual SNP or gene, all discriminatory SNPs are positionally clustered along the genome and used in a hierarchical selection algorithm to find the optimal SNP set which maximises the discriminatory power for each lineage, whilst minimising the number of amplicons required. Candidate regions are then used for multiplex PCR primer design, which can be validated *in silico* and *in vitro* before deployment (Figure 1).

Figure 1. Overview of Phylo-Plex workflow. 1 – Pathogen genome populations are analysed to determine SNPs that delineate individual lineages along ancestral branches. 2 – Discriminatory SNPs are clustered based on their genome position to identify information-rich candidate regions. 3 – Hierarchical selection of candidate regions maximises discrimination for each lineage whilst minimising the number of regions chosen. 4 – Selected regions are used for automated multiplex primer design. 5 – Primer designs are validated *in silico* to ensure the final scheme will amplify efficiently and without contamination, and that

genome population structures are accurately reconstructed. 6 – Primers are then optimized and validated in the laboratory using sequencing before deployment.

Identifying population structure defining SNPs

We constructed a globally representative dataset of 607 publicly available *T. pallidum* genomes, including high-quality genomes with ≥95% of reference positions at ≥5X coverage, and spanning *T. pallidum* subspecies *pallidum* (TPA, n=530), *T. pallidum* subspecies *pertenue* (TPE, n=75) and *T. pallidum* subspecies *endemicum* (TEN, n=2) (Supplementary Table 1). Sequencing reads were mapped to a common reference genome (NC_021508.1) and hypervariable and recombining regions were masked using an initial list of known recombinant genes, followed by *de novo* inference of recombination using Gubbins[18]. We inferred a whole genome phylogeny using IQ-tree[19,20], and designated phylogenetic sublineages using rPinecone[21] v0.1.0 with a threshold of up to 10 SNPs from the common ancestral node. This resulted in 40 sublineages and 33 singletons, including the 17 sublineages previously defined within TPA[15], and 23 newly-defined sublineages within TPE (Supplementary Figure 1).

Next, within this population structure we identified vertically inherited discriminatory SNPs by applying population genomic statistical tests of allelic segregation to a recombination-masked alignment, using Fixation Index[22] (F_{ST}) to define a list of SNPs that discriminate sublineages. Given that most *T. pallidum* genomic data are metagenomically derived and frequently contain uncertain genomic positions due to low coverage, this approach enabled delineation of informative SNPs whilst accommodating missing data. Retaining SNPs with F_{ST} ≥0.9, a combination of multiple SNPs together enables robust identification of each lineage or sublineage (Supplementary Figure 2). We applied this approach to each of the 40 sublineages defined in our population, as well as to delineate subspecies (TPA and TPE) and TPA major lineages (Nichols and SS14), resulting in a single list comprising 1549 discriminatory SNPs, of which 855 occurred on phylogenetic branches leading to individual sublineages, and thus discriminatory for sublineages, whilst the remaining 694 discriminatory SNPs fell on deeper branches and distinguished *T. pallidum* subspecies and major lineages (Supplementary Figure 3).

Examining the distribution of the 855 SNPs discriminating sublineages, we found that the number of SNPs along discriminatory branches of the phylogeny differed between sublineages (median 26 SNPs/sublineage, range 1-153; Supplementary Figure 4). Consistent with previous findings[15], the power to distinguish sublineages within the highly clonal SS14-lineage of TPA was limited (median 4 SNPs/sublineage, range 1-6). In contrast,

sublineages within Nichols-lineage TPA (median 20.5 SNPs/sublineage, range 7-60) and in TPE had much higher discrimination (median 39 SNPs/sublineage, range 16-153), reflecting more deeply branching sublineages in these parts of the phylogeny.

SNP refinement and hierarchical selection of candidate regions

To design an efficient amplicon scheme, we needed to optimise the choice of SNPs to maximise useful information whilst minimising the overall number of amplicons. To ensure multiplex PCR was efficient, we also needed to ensure amplicons were kept small (<1000 bp), and had similar lengths and melting temperatures. Examining the genomic positions of discriminatory SNPs, we found that although these SNPs were widely distributed across the genome for each sublineage (median 13,164 bp between SNPs, Supplementary Figure 5), they could be positionally clustered when analysed as a population (median 694 bp between SNPs). We evaluated the effect of clustering SNPs based on their genome position, forming network edges between SNPs based on different distance thresholds, and selected a distance of 300 bp since this clustered a high number of SNPs whilst keeping the majority of clusters below 1000 bp in length (Supplementary Figure 6). Of our initial 1549 discriminatory SNPs, 988 sites fell within 300 bp of at least one other discriminatory site, suggesting that this was an effective method for identifying localised phylogenetically information-rich regions of the genome (Figure 2A). Notably, we used *T. pallidum* here, which is highly genetically conserved with sparsely distributed SNPs across the core genome, limiting the available genomic sites which can be used for discrimination. In populations of pathogens with more diverse genomes, there would be more available SNPs and these may be more densely distributed, enabling simpler design with shorter clustering distances.

We constructed a network of clustered discriminatory SNPs using pairwise positional genome distances, allowing edges where SNPs were separated by ≤300 bp, and identifying 311 distinct network components, each containing >1 discriminatory sites (median 2, range 2-15) - henceforth referred to as ‘candidate regions’ (Figure 2B). For the remaining 561 discriminatory SNPs not included within a network component (i.e. singleton sites not positionally linked to another), we identified these as additional singleton regions, leaving a total of 872 candidate regions comprising 1549 individual SNPs. Of these, we excluded 50/872 larger candidate regions with total length ≥385 bp to minimise the PCR amplicon length, leaving 822 candidate regions.

Given the varying levels of SNP support for the different sublineages of TPA and TPE, we needed to optimise the number of potential amplicons whilst maintaining support for each

sublineage. We designed an algorithm to iteratively select candidate regions to maximise the number of discriminatory sites for each sublineage, whilst minimising the total number of regions included in the final scheme (Supplementary Figure 7). We considered the importance of maximising SNPs supporting each sublineage, whilst incorporating redundancy for PCR failures - aiming to avoid any single region being the sole supporter of a sublineage (which could lead to biases driven by hypervariable regions or residual recombination, as well as the risk of losing all support should PCR for that region fail).

Briefly, we constructed a ranked list of candidate regions based on the number of distinct sublineages supported by the SNPs within each region. Using an iterative loop, where initial support for each sublineage was considered to be zero regions, each candidate region was evaluated for its SNP support of specific sublineages. If a region contained SNPs that supported a sublineage, the counts for each supported sublineage were updated and the region was added to the scheme, unless the sublineage had already reached a minimum threshold of regions. For the *T. pallidum* scheme, we selected a minimum threshold of three regions, representing a compromise to provide robust discrimination whilst keeping the total number of amplicons small. Once a sublineage reached this threshold, new regions were not evaluated against it unless they contributed to another sublineage. To minimise potential biases driven by hypervariable regions or residual recombination, counts were increased by one for each sublineage supported by a candidate region even if that region contained multiple discriminatory sites to that sublineage. This process was repeated iteratively for all sublineages and regions. Consequently, our algorithm ensures all sublineages contain at least the minimum threshold discriminatory sites, unless there were fewer than this threshold initially available, whilst some sublineages (typically those representing more deeply branching lineages) contain more than the minimum (as subsequent sublineage picks may enrich discriminatory sites for other sublineages).

Our Phylo-Plex algorithm prioritised 76/822 candidate genomic regions that define the 40 sublineages within the dual global phylogenetic framework of TPA and TPE (Supplementary Figure 4). We re-examined the discriminatory power for each sublineage using this revised list and found that support for each sublineage was maintained, whilst the variability in terms of sites per sublineage was greatly reduced (mean 5.5 SNPs, range 1-48) (Supplementary Figure 4). To ensure similar PCR amplification dynamics and to make room for flanking primer design, we extended the length of each Phylo-Plex amplicon (we termed “Phy-cons”) to 700 bp by adding equal length flanking sequences to each end. We used these candidate regions for automated design of 20-24 bp primers with 59–63°C melting temperatures with PrimalScheme[10,11] (Supplementary Table 2), which produced 72 primer pairs with an

amplicon size distribution of 511-628 bp (4/76 candidate regions were unsuited to multiplex primer design and were excluded). We also designed and integrated a primer set for recovering the ribosomal 23S region (important for inferring antimicrobial resistance to macrolides in *T. pallidum* – in different pathogens, gene-specific markers for other resistance or virulence determinants could be used) to complete the final amplicon scheme of 73 Phy-cons. All 73 primer pair designs were initially evaluated for specificity using primer BLAST and *in silico* PCR (see Methods).

Figure 2. Positional clustering of discriminatory SNPs enables identification of information rich regions for PCR. A – Genomic distance between discriminatory SNPs for 40 sublineages. Blue line indicates 300 bp distance between sites. Black and Red points represent all discriminatory SNP-sites. Red points represent the clustered location-optimised SNPs represented in final amplicon panel design. B – Network showing the discriminatory SNPs coloured by the lineage they define and clustered by genome position. Nodes indicate individual SNPs and are coloured according to the sublineage supported. Edges indicate SNPs ≤ 300bp from each other, and form clusters of information-rich genomic regions. Red rings indicate clusters included in the final design.

Evaluation of laboratory sequencing and bioinformatics

Next, we evaluated the robustness of the laboratory and bioinformatic methods. We performed initial validation using ten-fold dilution series of genomic DNA extracted from four rabbit-passaged reference strains. We then selected 72 clinical swab samples from PCR-confirmed syphilis patients with a *Treponema* qPCR Ct between 23.9-32.2 from South Africa, and generated multiplex PCR amplicons in batches of 24 using the *Treponema* Phylo-Plex scheme (TP-Phylo-Plex). Because all Phy-cons were of a similar size, we used agarose gels to confirm overall pooled PCR performance, and sequencing coverage metrics to evaluate individual amplicon performance.

To ensure our scheme was easily and affordably deployable in low resource settings, we opted for MinION sequencing (Oxford Nanopore). We ligated individual sample barcodes to multiplex-PCR products once PCR success had been confirmed by gel electrophoresis, before pooling the barcoded PCR products and generating sequencing libraries. We used multiplex PCR products pooled from 24 individual samples as input for sequencing on MinION (Oxford Nanopore Technologies) Flongle flow cells, yielding 172,494-303,104 reads per run (after filtering of low quality <Q9, unmapped or reads outside of the accepted size range of 450-800bp) mapping to the targeted regions of the reference genome (NC_021508.1). This amounted to a median of 8,858 reads per sample (range 1,878-

20,414), distributed across 73 individual amplicons, with median coverage per amplicon of 104 (range 0-612) across the three sequencing runs and 72 samples.

Using read mapping coverage for each Phy-con, we found that 4/72 samples performed poorly with a mean coverage of <50X across all amplicons, and these were excluded from further analysis (Supplementary Figure 8). Notably, these four samples were not outliers in terms of Treponema qPCR - indeed the majority of South African samples performed well, suggesting the upper sensitivity limit for successful sequencing of the TP-Phylo-Plex assay was at least Ct 32 (Supplementary Figure 8).

Analysing coverage for individual Phy-cons, as expected amplicon recovery was improved for samples with increased pathogen load (determined by qPCR Ct; Supplementary Figure 9). However, 15/74 Phy-cons in the scheme consistently yielded reduced coverage in multiplex PCR (but performed well as single-plex PCR assays). For the purposes of the scheme development, we removed these amplicons and retrospectively evaluated the impact on discriminatory power for sublineages (Supplementary Figure 4), henceforth focussing on the 59 remaining Phy-cons that worked consistently in multiplex.

We next evaluated the sequencing accuracy of the Phy-cons generated for TP-Phylo-Plex on MinION. For this, we performed whole genome sequencing of the same 72 South African samples using the pooled sequence capture assay[3,15] on Illumina NovaSeq to provide a gold standard comparator (Supplementary Table 3). We obtained high quality (≥75% reference sites at ≥5X coverage) Illumina consensus genomes for 59 of the 68/72 samples which also had high Phy-con sequence coverage using MinION. Focusing on the regions of the whole genome represented by the Phy-cons, we directly compared the variant calls generated from these 59 samples by the two orthogonal sequencing methods, examining the 181 variable sites contained within the 59 Phy-cons for discordant results. Of these, we found perfect concordance for 179/181 variable sites across all samples. Of the two discrepant sites, the first (NC_021508.1 position 7002) affected 1/59 samples and was due to a deletion detected in the Illumina sequence (7002T) compared to the reference and MinION sequences (7002TG). On closer inspection, this was found to be a novel deletion present in both sets of sequencing reads, but was missed in the MinION sequencing because our pipeline did not correctly call INDELS. The second discrepancy (NC_021508.1 position 916096) occurred in 2/59 samples, and this site was found to be variable across the dataset (reference C allele, samples were either C or T). The two discrepant samples both had very low sequencing coverage in the relevant MinION sequencing amplicon and SNP loci (one mixed SNP with 2/3 reads supporting ‘T’; one clear ‘T’ allele supported by 6 reads). In both samples, this

discrepancy with the Illumina data was caused by insufficient read coverage from the MinION sequencing, leading to the variant caller failing to correctly call the SNP. To improve reproducibility and accessibility, we reimplemented the bioinformatics pipeline using NextFlow[23], and this included introducing additional quality steps around coverage that were designed to account for these issues in future.

Recapitulation of *T. pallidum* population structures by TP-Phylo-Plex

To assess the accuracy of phylogenetic delineation, we extracted the SNPs present within the final 59-amplicon scheme from a whole genome alignment and compared the resulting phylogeny to the one derived from the whole genomes (Figure 3). The distance matrices were correlated (Mantel statistic r=0.363, p<0.0001, 10,000 permutations), and we used Treespace[24] to demonstrate the trees were highly concordant with sublineage (concordance=0.900) compared to whole genome tree bootstraps (median concordance=0.337, 100 bootstraps) and whole genome tip-randomised trees (median concordance=0.188, 100 permutations) (Supplementary Figure 10).

Figure 3. Recapitulation of whole genome population structure using Phylo-Plex. Tanglegram comparing whole genome phylogeny with phylogeny calculated from the *in silico* predicted amplicons. Broad sublineage clustering is replicated in the vast majority of cases. Note, tree scales are not identical, since the branch lengths in the amplicon-derived tree were extended to illustrate differences; the underlying topologies were not changed.

Next, we evaluated TP-Phylo-Plex's ability to discriminate the 40 sublineages used in the original design. *In silico* evaluation of the original 73 amplicon design successfully delineated all 40 sublineages. However, the removal of 15 poorly performing amplicons resulted in a 59-Phy-con scheme which fully discriminated 31/40 sublineages. For the remaining 9 sublineages, three separate phylogenetic clades each comprising three related sublineages shared identical SNP patterns, and thus TP-Phylo-Plex could not distinguish within these three groups using the 59- Phy-con scheme (whilst still being clearly delineated from other sublineages) (Supplementary Figure 11). Notably, those sublineages occurred in clonal lineages such as TPA SS14-Lineage which had the smallest number of available discriminatory sites even at the WGS level, and were thus most affected.

We further evaluated the ability of TP-Phylo-Plex to discriminate previously described population structures, using a previously published whole genome phylogeny of 237 TPA

genomes from the UK[25] (Supplementary Figure 12). The dataset used for designing the scheme incorporated many of the same genomes and targeted the same sublineages, and TP-Phylo-Plex effectively recapitulated the population structure of UK syphilis.

Application in a low-resource setting

To determine the practical and operational feasibility of setting-up and using Phylo-Plex in a low resource setting, we set-up TP-Phylo-Plex at the Biomedical Research and Training Institute (BRTI; Harare, Zimbabwe), a small, ISO 15189 accredited service laboratory based in a converted townhouse. Equipment and molecular biology and sequencing reagents were shipped to Zimbabwe from the UK; key learning points here were around delays due to obtaining import permits. We implemented DNA extraction, qPCR diagnostics, multiplex PCR, library prep and sequencing on the MinION Flongle device (Oxford Nanopore Technologies) (Figure 4). We also performed full bioinformatic analysis using a Nextflow pipeline developed for processing Phy-con data, and real-time interpretation using an easy to use custom web app developed in Shiny (see Methods). We established realistic timelines for performing the assay in this setting, and were able to generate amplicons, perform sequencing and bioinformatics in under two days (Figure 4, Supplementary Table 4). As part of this process, two local PhD students were trained in all laboratory processes. Notably, power cuts occurred daily across Harare, but the BRTI laboratory had backup solar power cells. The backup system did malfunction, preventing PCR for two days. This highlights the need for robust power supply systems or qPCR machines that can run from batteries when using the method in a low resource setting.

Figure 4. Workflow and timelines for Phylo-Plex protocol. DNA is extracted from clinical swabs, before molecular diagnostics (multiplex qPCR). Confirmed PCR positive samples proceed to Phylo-Plex multiplex PCR and library preparation, before sequencing on MinION Flongle flowcells. Bioinformatic analysis is automated using a single command Nextflow pipeline and interpretation is performed using a web-based Shiny App.

For this field evaluation, we prospectively recruited 100 individuals with genital ulcers in Harare, Zimbabwe, as part of an ongoing multi-country research study investigating the aetiology of genital ulcers. Of 100 genital ulcer swabs collected, 14 were qPCR positive for *T. pallidum* (qPCR Cts range 21.9 – 35.3). We used the 59 Phy-con TP-Phylo-Plex assay to sequence the 14 samples (including technical replicates for two samples, and three replicates for one sample; Total 19), and recovered 12 complete TP-Phylo-Plex profiles (3 samples (5 replicates) with very high qPCR Ct >34 failed to amplify at sufficient depth)

(Supplementary Figure 13). This is consistent with our earlier observation that samples from South Africa performed well up to a qPCR Ct of 32, and suggests an approximate limit for successful sequencing between Ct 32 and 34.

Phylo-Plex offers a low-cost alternative for genomic surveillance

We evaluated the cost of implementing the 59-amplicon TP-Phylo-Plex, including all reagents (purchased in the UK using publicly displayed list prices) and consumables required for sequencing of PCR-positive DNA extracts. Excluding one-time setup costs (such as purchase of a sequencer and high-performance laptop), and assuming samples were sequenced in batches of 24, we estimated the cost to be £12.47/sample (Table 1). Of this cost, the most expensive components were the sequencing (£64.32/Flongle flow cell, £2.68/sample) and the native sample barcoding (£108.00/24 samples, £4.50/sample) reagents.

Future replacement of native barcoding by ligation with custom primers introduced during PCR would enable further cost savings, whilst sequencing in larger batches on higher capacity MinION flowcells (e.g. 96-384 plex) could reduce sequencing costs. Moreover, whilst the scheme used here implemented amplicons of approximately 700 bp, designing schemes with smaller amplicons (e.g. 300-400 bp) would allow for higher multiplexing of hundreds to thousands of samples on Illumina short-read sequencing platforms.

Table 1. Cost estimate for Phylo-Plex assay. Costs estimated using UK list pricing (institutional discounting may reduce this), and based on reagent volumes and usage. Initial setup costs may require larger purchases including MinION sequencer, High-performance laptop, Qubit Fluorometer, Thermocycler. Microcentrifuge, although many laboratories equipped for molecular biology, including those in Lower- and Middle Income Countries, may already have much of the required infrastructure (sometimes as a legacy of SARS-C0V-2 sequencing).

Component	Cost per 24 Samples (GBP)	Cost per Sample (GBP)
Reagents		
Q5 Hot Start High-Fidelity 2X Master Mix (100)	£11.76	£0.49
NEBNEXT Ultra II End Repair/dA-tailing module (96)	£35.28	£1.47
NEB Blunt/TA Ligase Master Mix (250)	£44.40	£1.85
NEBNext Quick Ligation Module (20)	£20.40	£0.85
Agarose / loading dye / EtBr / ladder	£1.56	£0.07
ONT Native Barcoding Kit 24 V14	£108.00	£4.50

Qubit dsDNA HS Assay Kit (500 rxns)	£1.48	£0.06
PCR Primers	£4.32	£0.18
ONT Flongle Flow Cell	£64.32	£2.68
Reagent Total (Assuming List Prices)	**£291.52**	**£12.15**
Plasticware		
Qubit Assay Tubes	£1.96	£0.08
Microfuge Tubes	£0.30	£0.01
PCR Tubes	£0.52	£0.02
Filter Tips	£5.00	£0.21
Plasticware Total (Assuming List Prices)	**£7.78**	**£0.32**
Total Assay Cost	**£299.30**	**£12.47**

Future proofing the Phylo-Plex and the Phy-con design

Although Phylo-Plex was specifically optimised to recover known population structures and sublineages, our approach of retaining and using SNP information means that detection of novel SNPs and sublineages is theoretically possible, provided the genomic variants occur within the targeted amplicon regions. We originally used rPinecone to cluster *T. pallidum* sublineages on the basis of being within 10-SNPs from a common ancestral node[21], meaning that individual genomes within the same sublineage can be separated by up to 20 SNPs. Within the TP-Phylo-Plex amplicons, representing approximately 3.6% of the genome, most samples from the same sublineage were identical or differed by a single SNP (Supplementary Figure 11). Detection of a novel sublineage using TP-Phylo-Plex would therefore require at least two novel SNPs occurring within the available Phy-cons. Notably, *T. pallidum* accumulates approximately one substitution per genome every 7 years[15], and novel sublineages with sufficient SNPs divergence for detection using TP-Phylo-Plex would therefore also be epidemiologically distinct.

Next, to quantify the sensitivity of TP-Phylo-Plex to novel variation, we simulated vertically inherited (non-recombining) SNPs accumulating in the genome by introducing random *in silico* mutations to the 1.139 Mb *T. pallidum* genome at different frequencies (0.1%, 0.05%, 0.01%, 0.005%, 0.001%, 0.0005%), corresponding to defined SNPs/genome (1140, 570, 114, 57, 11, 6). We counted how many WGS mutations occurred within TP-Phylo-Plex

amplicons, evaluating each mutational frequency over 250 simulations, and found that at 0.001% genomic sites mutated (11 SNPs/genome – similar to the discriminatory level within our sublineages), only 5.2% of simulations had ≥2 SNPs occurring within the 59-amplicon TP-Phylo-Plex scheme. However, this increased to 45.6% of simulations at 0.005% genome sites mutated (57 SNPs) and to 87.6% of simulations at 0.01% genomic sites (114 SNPs) (Supplementary Figure 14). Therefore, the probability of distinguishing a novel sublineage depends on the level of genetic divergence – substantially divergent novel sublineages separated by >100 SNPs have a high probability of being identified, whilst the probability is reduced with less divergent sublineages. This is similar to how a standard MLST scheme would detect a new sequence type, except Phylo-Plex captures a larger proportion of the genome, and therefore has greater opportunity to detect novelty.

Should novel diversity be identified (either through Phylo-Plex, or through more conventional WGS surveillance), a further consideration is how straightforward it would be to enhance detection of novel diversity through adding additional amplicons. Notably, PCR primers represent a very small fraction of total assay costs – including a small number of additional primers would have minimal cost implications. However, since the primers are designed to work together in a multiplex, new primers would need to be validated *in silico* to ensure they were compatible with existing primers, as well as *in vitro* to ensure the multiplex PCR still functioned correctly. A simpler and more flexible solution would be to add a second more locally or regionally targeted multiplex PCR including new Phy-cons. This same approach could also be used for tracking non-chromosomal elements such as plasmids or AMR genes. The PCR products of both multiplexes could be combined before library preparation, at an estimated additional cost of £0.67/sample (Table 1), largely driven by the reagent costs of performing a second PCR. Alternatively, these secondary primer sets could simply be deployed on samples showing variation in the more general Phylo-Plex amplicon set.

Discussion

As genomic surveillance becomes routine in high income countries, there is a need to maximise the utility of global microbial whole genome data we generate as a community so it can be used for epidemiological tracking in all settings. As a consequence of the international SARS-CoV-2 response, multiplex amplicon sequencing is now a proven technology widely used by laboratories around the world[11]. We sought to build on this capacity by developing a novel approach which enables low-cost and adaptable sequence-based pathogen surveillance in all settings, including those that are resource poor[26].

In the UK, Illumina sequencing of bacterial genomes is offered commercially in the region of £65/sample, and typically makes use of high throughput sequencers to reduce per-sample costs, requiring large batches of samples to make them affordable for pathogen sequencing. This can impact the timeliness of results whilst awaiting sufficient samples to complete a batch. Alternatives such as MLST are sometimes perceived as a cheaper alternative, but a typical MLST scheme uses 7 amplicons and requires 14 Sanger sequencing reads/sample, available at £2-£8/reaction commercially. Therefore, MLST costs £28-£112/sample. By comparison, our TP-Phylo-Plex protocol costs £12.47/sample, and still recapitulates the current global population structure derived from whole genomes with a high degree of precision. Moreover, Phylo-Plex can be run in small batches (<£300/24 sample run) and give results in 24-48 hours, but because it can use multiple sequencing technologies, it can be scaled to enable very high throughput (hundreds of samples/run) sequencing. This makes it ideal for deployment to investigate emerging outbreaks *in situ* as well as more long-term surveillance studies.

We chose *T. pallidum* as a model pathogen because it is extremely expensive and complicated to culture, syphilis is a major global health concern and there is still limited data on its global diversity and spread. Moreover, Phylo-Plex is particularly attractive for *T. pallidum* because of the need to use costly metagenomic methods to recover genomes, as well as low genetic diversity and minimal recombination which made design against a reference genome straightforward. However, the Phylo-Plex method is also appropriate for low-cost genomic surveillance of viral, bacterial and fungal pathogens, and because of the robust and portable nature of the method, as well as the relative ease of laboratory training, is ideally suited and proven for use in low resource settings, enabling tracking of diseases of public health importance such as mpox, chlamydia, typhoid, and cholera.

Unlike traditional molecular typing methods, Phylo-Plex uses population genomics-informed, phylogenetically robust grouping of taxa within specie(s). Inspired by computational hierarchical SNP typing methods such as GenoTyphi[27], we developed an approach that focuses on key ancestral SNPs for clustering genomes, but refined the concept using network approaches to reduce operational complexity and design a low-cost laboratory method suitable for all settings. Despite recovering only 3.6% of the total genome length, our TP-Phylo-Plex scheme showed high concordance with the whole genome phylogeny, and indeed showed higher concordance than bootstrapped datasets derived from the whole genome itself. Moreover, our laboratory validation showed high accuracy in SNP detection, supporting our use of nanopore sequencing for field deployment.

Phylo-Plex can be used both as a standalone surveillance tool, and also to supplement and extend whole genome sequencing approaches; for a given population, a subset of samples could undergo WGS to identify key lineages, followed by design of a Phylo-Plex scheme to enable scaleup, and we describe important steps for how new schemes can be developed and evaluated before deployment. Existing Phylo-Plex schemes could also be rapidly adapted to a new outbreak simply by adding a separate pool of amplicons. Importantly, the sensitivity of a Phylo-Plex scheme can be adjusted – we removed 15/74 amplicons from the TP-Phylo-Plex for operational reasons, yet this still enabled full delineation of 31/40 known sublineages. Moreover, Phylo-Plex is capable of detecting novel lineages, albeit this is largely dependent on the level of nucleotide divergence between lineages. Adding more amplicons offers greater resolution and can enable antimicrobial resistance or virulence genotyping, at minimal additional cost, but this must be balanced against the technical complexity and time to optimise. The sensitivity required can be judged according to whether a particular lineage or sublineage, detectable by WGS and circulating in relevant populations, is of sufficient clinical relevance to require discrimination from other lineages. A recent example would be the current global health emergency associated with mpox lineage 1b which may have distinct disease outcomes[28], where being able to rapidly and cheaply discriminate the causal lineage in an outbreak can inform both public health management and patient treatment.

Methods

In silico methods and design

Dataset preparation

We constructed a globally representative dataset of 607 publicly available *Treponema pallidum* genomes, including high quality genomes with ≥95% of reference positions at ≥5X coverage. The vast majority of these had been sequenced using the pooled sequence capture method on an Illumina sequencer[3] (Supplementary Table 1). Sequencing reads were mapped to a common reference genome (SS14, NC_021508.1), and masked for previously described hypervariable, repetitive and recombining genes, as well as using Gubbins[18] v2.4.1 to further identify and filter recombining regions as previously described[15]. From the resulting multiple sequence alignment, we then constructed a maximum likelihood phylogeny

using IQ-Tree[19,20] v1.6.12, and inferred phylogenetic sublineages using rPinecone[21] v0.1.0 with a threshold of up to 10 SNPs from the common ancestral node.

Identifying and refining discriminatory sites

We converted whole genome sequence alignments into Variant Call Format (VCF) using snp-sites[29] v2.5.1, before importing the data into R using vcfR[30] v1.15.0. We created binary matrices for each genome indicating membership of each sublineage. We also included comparisons for *T. pallidum* subspecies (*pallidum* and *pertenue*), as well as the subspecies *pallidum* major lineages Nichols and SS14. For each sublineage, we then tested each variable SNP for population segregation using Weir and Cockerham's F_{ST}, using the `wc` command in hierfstat[31] v0.5.11. We considered sites with $F_{ST} \geq 0.90$ sufficient for downstream analysis. Since our analysis included sites masked to 'N', we identified and excluded sites where the 'N' could potentially be misrepresented as a discriminatory SNP.

To identify information-rich regions of the genome, we calculated pairwise positional distances between discriminatory SNPs. We then subset data to include distances below individual thresholds, testing 50 bp intervals from 50-1000 bp. For each set of distances, we formed edge networks using the network package v1.18.2 in R, and extracted network components using iGraph v2.0.3, counting the number of network components (genomic regions), as well as the number of discriminatory SNPs per region and size range of the regions. Note that this approach of linking individual SNPs by distance can result in chains of connected SNPs that span many thousands of bases. Increasing the size of the linkage interval results in more SNPs within a network component, but increasingly leads to longer amplicons. We selected 300 bp for linkage as optimal for *T. pallidum*, since this balanced network components and SNP count against region size.

Primer design

For multiplex primer design, we used the command line version of PrimalScheme[10,11] v1.3.2, using the option to supply multiple distinct alignments for combined primer design. Using the SS14 reference genome (NC_021508.1), we generated a representative pseudomolecule, where genomic positions in our genome collection that were variable in ≥0.5% of genomes were masked to 'N'. We then extracted target regions into individual fasta files, with the target region itself masked to 'N', and flanked by 150bp unmasked sequence. We specified a target amplicon size of 684bp (selected due to the typical target region size and allowing for flanking regions) in PrimalScheme to ensure multiplex primer design was forced to occur around the masked target region. We used the standard GC content and specified predicted melting temperatures of 59–63°C [10]. All primers were evaluated *in silico* using primer

BLAST[32] (implemented in primerTree[33] v1.0.6), as well as using *in silico* PCR (available at https://github.com/sanger-pathogens/sh16_scripts/blob/master/legacy/in_silico_pcr.py) against SPAdes[34] assemblies of the genome data.

Macrolide resistance primer design

Macrolide resistance in *T. pallidum* is mediated by point mutations (A2058G, A2059G) in the ribosomal 23S sequences. Although published primers for *Treponema* 23S exist[35,36], these were not optimised for compatibility with the multiplex scheme, necessitating design of new primers. To identify highly conserved *Treponema* specific regions in the 23S gene, which occurs universally at high homology across bacteria, we performed Compact Bit-Sliced Signature Index[37] (COBS) search against a collection of ~661,000 uniformly assembled bacterial genomes[38]. We used the *T. pallidum* ribosomal operon as a template, and generated 71 bp sliding windows along the *Treponema* operon as queries for COBS, examining identical (100%) search hits from the full bacterial dataset. The median genome count for each window was 129 (reflecting the number of *T. pallidum* genomes in the dataset), and regions of the *T. pallidum* 23S operon identified as matching ≥5% above the median (135.5) were flagged as potentially cross-species matches and masked to avoid use in primer design. This was confirmed by examining the species identities of the hits. Unmasked regions were used as input to PrimalScheme for primer design using the conditions described for the full discriminatory scheme, and final primer designs were screened using primer BLAST.

In silico validation

To evaluate the scheme, we initially simulated amplicons from Illumina-derived whole genomes. Based on the target regions, we extracted SNPs and constructed multiple sequence alignments using the vcfR[30] v1.15.0, ape[39] v5.8 and seqinr[40] v4.2.36 packages, from which we inferred phylogenies using IQ-Tree[19] v1.6.12. We compared the whole genome phylogenies to the inferred amplicon phylogenies for phylogenetic consistency using tanglegrams produced using ggtree[41] v3.12.0, distance matrix comparison using Mantel tests in the vegan[42] v2.6.6.1, as well as correlating whole genome derived sublineages with amplicon derived phylogenies using the treeConcordance function in Treespace[24] v1.1.4.3. We examined distinct sublineage clustering by constructing networks of identical amplicon profiles, and correlating these with WGS-derived sublineage assignments in R. We subsequently performed direct comparisons on Illumina whole genome and MinION amplicon variant calls and phylogenetic placement derived from the same samples by integrating the variant calls from both methods (described below) using bcftools merge[43] v1.19.

To evaluate the ability of Phylo-Plex to detect novel variation, we used a custom python script (randomly_mutate_genome.py, available at https://github.com/matbeale/TP-Phylo-Plex_paper_2025) to introduce random mutations at defined frequencies (0.1%, 0.05%, 0.01%, 0.005%, 0.001%, 0.0005%) into the SS14 reference genome (NC_021508.1). We simulated 250 different mutated genomes at each frequency, and converted the resulting fasta files to multi-sample variant call files (VCF) using snp-sites. We imported VCFs into R using vcfR and partitioned the SNPs for each simulated genome. For each set of variants, we calculated how many intersected with the amplicon positions using iRanges[44] v2.38.0 and created summary statistics using tidyverse[45] v2.0.0.

Laboratory workflow

Validation samples

For initial validation of PCRs, we used ten-fold dilution series of high copy number rabbit passaged strains (SEA-83-1, BAL-2, BAL-6, Haiti-B). We also used a clinical dataset of 72 syphilis swab DNA samples derived from patients with genital ulcers in South Africa, which were sequenced using both Illumina (pooled sequence capture[3]) and the Phylo-Plex method. We also prospectively recruited 100 patients with genital ulcers in Zimbabwe as part of an ongoing study ("Multi-country Aetiology of Genital Ulcer Survey" – MAGUS); 14 *T. pallidum* PCR-positive swab DNA samples were sequenced using the protocol in a low-resource laboratory at the Biomedical Research and Training Institute in Harare, Zimbabwe. This included two samples independently extracted and sequenced as technical replicates; for one of these samples, we also sequenced the same extract twice as a further technical replicate.

PCR amplification

We modified the ARTIC network (https://artic.network/) SARS-CoV-2 sequencing protocol (available at https://www.protocols.io/view/artic-sars-cov-2-sequencing-protocol-v4-lsk114-bp2l6n26rgqe/v4) for multiplex PCR and library preparation, adjusting reaction volumes to reduce cost and increasing cycling times to improve PCR efficiency of 700 bp amplicons. Briefly, for each sample we prepared a PCR reaction mix containing 6.25µl Q5 Hot Start High-Fidelity 2X Master Mix (New England Biolabs), 2µl pooled multiplex primers (10 mM; Integrated DNA Technologies), 1.75µl nuclease-free water, and 2.5µl template DNA (total reaction volume of 12.5µl). Samples were initially denatured for 30 seconds at 98°C, followed by 35 cycles of 15 seconds at 98°C, 4 ½ minutes at 62°C and 30 seconds at 72°C.

Performance of bulk PCR products was assessed using agarose gels, ensuring a band was present at 700-800 bp.

Library preparation and sequencing

PCR products were used directly without cleanup, and diluted 1:5 (or less, if fewer than 24 samples/run) in nuclease-free water. We performed end repair using the NEBNext Ultra II End Prep module (New England Biolabs), combining 1.2 µl Ultra II End Prep buffer with 0.5µl End Prep Enzyme Mix, and adding 8.3µl of diluted PCR product, before incubation for 15 minutes at room temperature (~20°C), then inactivation for 15 minutes at 65°C, then 1 minute on ice. PCR products were individually barcoded using 5µl Blunt/TA Ligase Master Mix (New England Biolabs), 1.25µl DNA barcode (EXP-NBD104, EXP-NBD114 or EXP-NBD196; Oxford Nanopore Technologies), 3µl nuclease-free water, and 0.75µl end-repaired product from the previous step; ligation reactions were incubated for 20 minutes at room temperature, followed by 10 minutes at 65°C, then 1 minute on ice. All barcoded PCR products were then pooled into a single tube for onward preparation. We performed two rounds of SPRI bead cleanup (AmpureXP, Beckman-Coulter) at 0.4X, using the Short Fragment Buffer for washing (Oxford Nanopore Technologies). After cleanup and quantification, we ligated sequencing adaptors (Oxford Nanopore Technologies) by combining 10µl NEBNext Quick Ligation Reaction Buffer (5x), Quick T4 DNA Ligase (both New England Biolabs), 5µl Native Adaptor (Oxford Nanopore Technologies), and 30µl pooled library, followed by incubation for 20 minutes at room temperature. We then performed two further rounds of SPRI bead cleanup, before final quality control and library preparation.

Pooled multiplex amplicon libraries were sequenced in groups of 24 on a single run of the MinION Flongle device (Oxford Nanopore Technologies) using either R9.4.1 (initial validation and testing of South African samples) or R10.4.0 (field deployment and Zimbabwe samples) chemistry, with the change motivated by discontinuation of R9.4.1 reagents and flowcells. Where fewer than 24 samples were available (e.g. in Zimbabwe), we reduced the dilution factor of initial PCR products from 1:5 up to 1:3 to ensure sufficient total DNA was available for subsequent steps.

Bioinformatic analyses

Basecalling, QC, Variant calling

Illumina data was processed and analysed as previously described[15]. Briefly, enriched metagenomic sequencing reads were screened using Kraken2[46] v2.1.2 and *Treponema* reads were extracted using seqtk v1.3 (available at https://github.com/lh3/seqtk). We

mapped sequencing reads to the SS14 reference (NC_021508.1) after masking previously described recombinogenic regions, called variants using bcftools[43] v1.19 to construct a multiple sequence alignment, and used Gubbins[18] v2.4.1 to identify and mask additional recombinant sites.

Initial validation of MinION amplicon data was conducted using a custom pipeline. Sequencing runs were basecalled and demultiplexed using the high accuracy model in Guppy v6.4.2. Sequencing reads with >Q9 were mapped to the SS14 reference (NC_021508.1) using minimap2[47] v2.16, and quality metrics were produced using samtools[48]. In particular, we calculated coverage metrics for each individual amplicon by parsing the outputs of samtools depth v1.6. After mapping, we trimmed reads to remove primers using Cutadapt[49] v1.15, before performing SNP calling using Clair3[50] v1.0.1 (available at https://github.com/HKU-BAL/Clair3). We compared variants inferred from Nanopore data to Illumina data by merging filtered VCF files using bcftools[43] v1.19.

After initial validation of methods, we subsequently reimplemented this workflow in a streamlined NextFlow[23] pipeline (available at https://github.com/sanger-pathogens/long-read-ampliseq; workflow shown in Supplementary Figure 15). This replaced the basecaller with Dorado v0.5.1 (available at https://github.com/nanoporetech/dorado), incorporated additional quality steps, and refined variant calling and pseudosequence generation. Raw sequencing reads (fast5/pod5) were base-called using Dorado with the "dna_r10.4.1_e8.2_400bps_hac@v4.3.0" model and minimum quality score set to 9, and demultiplexed using the appropriate barcode kit name specified (e.g. 'SQK-NBD114-24'). samtools[48] v1.19.2 was used to convert the resulting bams to fastqs. Primers and low quality (below Q15 at each end) bases were trimmed from fastqs using Cutadapt[49] v4.7, with lower read length cutoff set to 450 and upper read length cutoff set to 800 to ensure only reads of the expected length were included. Remaining bases with quality <15 were also masked using seqtk v1.4 (available at https://github.com/lh3/seqtk). Mapping of the reads against the masked SS14 reference was performed using Minimap2[47] v2.26. Unmapped reads and alignments with mapping quality below 50 were filtered using samtools[48]. As each read should map to one of the target regions, alignments not overlapping with these regions or that are secondary or supplementary were also filtered. Variant calling was performed using Clair3[50] v1.0.9 in haploid mode, using the "r1041_e82_400bps_hac_v430" model and specifying to only call SNPs with a minimum coverage of 5. Bcftools[43] v1.20 was used to merge the genome variant call files (gvcfs) from all samples to a multi-sample vcf and also to convert to tab-delimited format for simple parsing. A custom script run in Python 3.10.12 (available in the pipeline) was used to create a consensus fasta file for each sample with

individual target regions, as well as all the target regions concatenated, including variants and reference calls with minimum genotype quality of 1 and masking everything else. Individual target region fastas were also concatenated to make a multiple sequence alignment, from which SNPs were extracted with snp-sites[29] v2.5.1. Throughout the pipeline, various tools are used for QC reporting at different stages, including PycoQC v2.5.2 (available at https://github.com/a-slide/pycoQC), FastQC[51] v0.12.1 (available at https://github.com/s-andrews/FastQC), samtools, bedtools v2.31.1, as well as custom Python scripts. MultiQC[52] v1.22.2 is used to create a summary report combining output from PycoQC, FastQC and samtools stats/flagstat for all samples. Typical run time for this pipeline on a high-performance laptop for a TP-Phylo-Plex MinION Flongle sequencing run was 20-40 minutes (depending on the number of reads generated by the sequencing). Fieldwork in Zimbabwe used https://github.com/sanger-pathogens/long-read-ampliseq v1.0.0 for analysis.

We also developed a Shiny web interface ("AmpliSeq_QC_Frontend.R") in R which can be loaded using Rstudio, included with the pipeline code at https://github.com/sanger-pathogens/long-read-ampliseq, to enable straightforward guided interpretation of bioinformatics outputs for use by non-bioinformaticians in the field. This takes the directory path of a completed NextFlow pipeline run as input, and provides a point-and-click interface to assess quality and coverage metrics, allowing the user to select and deselect samples, and reanalysing results (including phylogenies and plots) in real-time.

Statistics and plotting

Phylogenies and tanglegrams were plotted using ggtree[41] v3.12.0, and all other plots were produced using ggplot2[53] v3.5.1 in R[54] v4.4.2. Networks were plotted using ggnetwork[55] v0.5.13 and iGraph[56] v2.0.3, and all statistics were calculated in R. Code workflows were made in draw.io and Lucidchart. Additional diagrams were made in Inkscape. ChatGTP v3.5 was used for initial code scaffolding and to assist with troubleshooting during the development of the Shiny application for Nextflow data interpretation.

Ethical approvals

Clinical samples from South Africa were collected as part of routine public health surveillance, and ethical approval for genome sequencing was granted by the University of the Witwatersrand Human Research Ethics Committee (Medical) (Ethics clearance certificate no. M230157). Clinical swabs from Zimbabwe were collected as part of the Multi-Country Aetiology of Genital Ulcer Study (MAGUS), and ethical approvals were granted for patient recruitment, diagnostics and genomics from the Medical Research Council of

Zimbabwe (MRCZ/A/2878), the Biomedical Research and Training Institute Institutional Review Board (Ap/175/2022) and the London School of Hygiene and Tropical Medicine Ethics Committee (26731).

Data and Code Availability

European Nucleotide Archive (ENA) Accessions for Illumina sequencing reads from the initial dataset used for primer design are listed in Supplementary Table 1. Accessions for the Illumina reads from South African syphilis are listed in Supplementary Table 3 and are available at the ENA under project accession PRJEB60271. Oxford Nanopore sequencing reads are available from the ENA under project accession PRJEB85457, and are listed in Supplementary Table 3 (for South Africa) and Supplementary Table 4 (for Zimbabwe).

The code used in this paper (including for identifying discriminatory sites and the hierarchical selection algorithm) are available at https://github.com/matbeale/TP-Phylo-Plex_paper_2025 and at https://doi.org/10.5281/zenodo.14894111. The Nextflow pipeline for automated data processing of Phylo-Plex data is available at https://github.com/sanger-pathogens/long-read-ampliseq.

Author Contributions

Conceptualisation: MAB; Methodology: MAB, VS, KEA, GL, SD, WRS, BS, FL, MJD; Formal Analysis: MAB; Investigation: MAB, VS, KEA, GL, MC, TMW; Resources: MAB, SD, WRS, BS, FL, MPM, JMEV, BDCD, EM, LR, BM, MM, NRT; Data Curation: MAB, VS; Writing – Original Draft: MAB; Visualisation: MAB; Supervision: LR, RAF, NRT; Project Administration: MAB, MM, BM, ED, EM, RAF, NRT.

Acknowledgements

We thank the teams and administrators at the National Institute for Communicable Disease in South Africa and at the Zvitambo and Biomedical Research and Training Institute labs in Harare, Zimbabwe, as well as all partners involved in the MAGUS study. We acknowledge the Core Sequencing, Pathogen Informatics and Samples teams at the Wellcome Sanger Institute.

This work was part-funded by a Gates Foundation grant (INV-035896) to MAB, MM, RAF and NRT. MAB, VS, KEA, GL, SD, WRS, BS, FL, MJD and NRT were supported by Wellcome funding to the Sanger Institute (206545/Z/17/Z).

This work was supported, in whole or in part, by the Gates Foundation [INV-035896] and the Wellcome Trust [206545/Z/17/Z]. The conclusions and opinions expressed in this work are those of the authors alone and shall not be attributed to the Gates Foundation or the Wellcome Trust. Under the grant conditions of the Foundation, a Creative Commons Attribution 4.0 License has already been assigned to the Author Accepted Manuscript version that might arise from this submission. Please note works submitted as a preprint have not undergone a peer review process.

References

1. Gardy, J. L. & Loman, N. J. Towards a genomics-informed, real-time, global pathogen surveillance system. *Nat. Rev. Genet.* nrg.2017.88 (2017) doi:10.1038/nrg.2017.88.
2. Struelens, M. J. *et al.* Real-time genomic surveillance for enhanced control of infectious diseases and antimicrobial resistance. *Front. Sci.* **2**, (2024).
3. Beale, M. A. *et al.* Genomic epidemiology of syphilis reveals independent emergence of macrolide resistance across multiple circulating lineages. *Nat. Commun.* **10**, 3255 (2019).
4. Hadfield, J. *et al.* Comprehensive global genome dynamics of Chlamydia trachomatis show ancient diversification followed by contemporary mixing and recent lineage expansion. *Genome Res.* **27**, 1220–1229 (2017).
5. Uelze, L. *et al.* Typing methods based on whole genome sequencing data. *One Health Outlook* **2**, 3 (2020).
6. Luo, Y. *et al.* US Gulf-like toxigenic O1 *Vibrio cholerae* causing sporadic cholera outbreaks in China. *J. Infect.* **72**, 564–572 (2016).
7. Grillová, L. *et al.* Molecular characterization of Treponema pallidum subsp. pallidum in Switzerland and France with a new multilocus sequence typing scheme. *PloS One* **13**, e0200773 (2018).
8. Lieberman, N. A. P. *et al.* Treponema pallidum genome sequencing from six continents reveals variability in vaccine candidate genes and dominance of Nichols clade strains in Madagascar. *PLoS Negl. Trop. Dis.* **15**, e0010063 (2021).

9. Quick, J. nCoV-2019 sequencing protocol. (2020).
10. Quick, J. *et al.* Multiplex PCR method for MinION and Illumina sequencing of Zika and other virus genomes directly from clinical samples. *Nat. Protoc.* **12**, 1261–1276 (2017).
11. Kent, C. *et al.* PrimalScheme: open-source community resources for low-cost viral genome sequencing. 2024.12.20.629611 Preprint at https://doi.org/10.1101/2024.12.20.629611 (2024).
12. Plante, J. A. *et al.* The variant gambit: COVID-19's next move. *Cell Host Microbe* **29**, 508–515 (2021).
13. WHO. Syphilis. https://www.who.int/news-room/fact-sheets/detail/syphilis.
14. Edmondson, D. G., Hu, B. & Norris, S. J. Long-Term In Vitro Culture of the Syphilis Spirochete *Treponema pallidum* subsp. *pallidum*. *mBio* **9**, e01153-18 (2018).
15. Beale, M. A. *et al.* Global phylogeny of Treponema pallidum lineages reveals recent expansion and spread of contemporary syphilis. *Nat. Microbiol.* **6**, 1549–1560 (2021).
16. Taouk, M. L. *et al.* Characterisation of Treponema pallidum lineages within the contemporary syphilis outbreak in Australia: a genomic epidemiological analysis. *Lancet Microbe* **3**, e417–e426 (2022).
17. Seña, A. C. *et al.* Clinical and genomic diversity of Treponema pallidum subspecies pallidum to inform vaccine research: an international, molecular epidemiology study. *Lancet Microbe* **0**, (2024).
18. Croucher, N. J. *et al.* Rapid phylogenetic analysis of large samples of recombinant bacterial whole genome sequences using Gubbins. *Nucleic Acids Res.* gku1196 (2014) doi:10.1093/nar/gku1196.
19. Nguyen, L.-T., Schmidt, H. A., von Haeseler, A. & Minh, B. Q. IQ-TREE: A Fast and Effective Stochastic Algorithm for Estimating Maximum-Likelihood Phylogenies. *Mol. Biol. Evol.* **32**, 268–274 (2015).
20. Minh, B. Q. *et al.* IQ-TREE 2: New Models and Efficient Methods for Phylogenetic Inference in the Genomic Era. *Mol. Biol. Evol.* **37**, 1530–1534 (2020).

21. Wailan, A. M. *et al.* rPinecone: Define sub-lineages of a clonal expansion via a phylogenetic tree. *Microb. Genomics* (2019) doi:10.1099/mgen.0.000264.

22. Weir, B. S. & Cockerham, C. C. Estimating F-Statistics for the Analysis of Population Structure. *Evolution* **38**, 1358–1370 (1984).

23. Di Tommaso, P. *et al.* Nextflow enables reproducible computational workflows. *Nat. Biotechnol.* **35**, 316–319 (2017).

24. Jombart, T., Kendall, M., Almagro-Garcia, J. & Colijn, C. treespace: Statistical exploration of landscapes of phylogenetic trees. *Mol. Ecol. Resour.* **17**, 1385–1392 (2017).

25. Beale, M. A. *et al.* Genomic epidemiology of syphilis in England: a population-based study. *Lancet Microbe* **4**, e770–e780 (2023).

26. Wilson, C. N., Musicha, P. & Beale, M. A. Genomic epidemiology on the move. *Nat. Rev. Microbiol.* 1 (2022) doi:10.1038/s41579-022-00836-4.

27. Wong, V. K. *et al.* An extended genotyping framework for Salmonella enterica serovar Typhi, the cause of human typhoid. *Nat. Commun.* **7**, 12827 (2016).

28. Beiras, C. G. *et al.* Concurrent outbreaks of mpox in Africa—an update. *The Lancet* (2024) doi:10.1016/S0140-6736(24)02353-5.

29. Page, A. J. *et al.* SNP-sites: rapid efficient extraction of SNPs from multi-FASTA alignments. *Microb. Genomics* **2**, (2016).

30. Knaus, B. J. & Grünwald, N. J. vcfr: a package to manipulate and visualize variant call format data in R. *Mol. Ecol. Resour.* **17**, 44–53 (2017).

31. Goudet, J. & Jombart, T. hierfstat: Estimation and Tests of Hierarchical F-Statistics. (2022).

32. Altschul, S. F., Gish, W., Miller, W., Myers, E. W. & Lipman, D. J. Basic Local Alignment Search Tool. *J. Mol. Biol.* **215**, 403–410 (1990).

33. Hestor, J. & Cannon, M. primerTree: Visually Assessing the Specificity and Informativeness of Primer Pairs. (2022).

34. Bankevich, A. *et al.* SPAdes: A New Genome Assembly Algorithm and Its Applications to Single-Cell Sequencing. *J. Comput. Biol.* **19**, 455–477 (2012).

35. Grimes, M. *et al.* Two Mutations associated with Macrolide Resistance in Treponema pallidum: Increasing Prevalence and Correlation with Molecular Strain Type in Seattle, Washington. *Sex. Transm. Dis.* **39**, 954–958 (2012).

36. Beale, M. A. *et al.* Yaws re-emergence and bacterial drug resistance selection after mass administration of azithromycin: a genomic epidemiology investigation. *Lancet Microbe* **1**, e263–e271 (2020).

37. Bingmann, T., Bradley, P., Gauger, F. & Iqbal, Z. COBS: A Compact Bit-Sliced Signature Index. in *String Processing and Information Retrieval* (eds. Brisaboa, N. R. & Puglisi, S. J.) 285–303 (Springer International Publishing, Cham, 2019). doi:10.1007/978-3-030-32686-9_21.

38. Blackwell, G. A. *et al.* Exploring bacterial diversity via a curated and searchable snapshot of archived DNA sequences. *PLOS Biol.* **19**, e3001421 (2021).

39. Paradis, E. & Schliep, K. ape 5.0: an environment for modern phylogenetics and evolutionary analyses in R. *Bioinformatics* **35**, 526–528 (2019).

40. Charif, D. & Lobry, J. Seqin{R} 1.0-2: a contributed package to the {R} project for statistical computing devoted to biological sequences retrieval and analysis. in *Structural approaches to sequence evolution: Molecules, networks, populations* (eds. Bastolla, U., Porto, M., Roman, H. & Vendruscolo, M.) 207–232 (Springer-Verlag, New York, 2007).

41. Yu, G., Smith, D. K., Zhu, H., Guan, Y. & Lam, T. T.-Y. ggtree: an r package for visualization and annotation of phylogenetic trees with their covariates and other associated data. *Methods Ecol. Evol.* **8**, 28–36 (2017).

42. Oksanen, J. *et al.* vegan: Community Ecology Package. R Package. (2015).

43. Danecek, P. & McCarthy, S. A. BCFtools/csq: haplotype-aware variant consequences. *Bioinformatics* **33**, 2037–2039 (2017).

44. Lawrence, M. *et al.* Software for Computing and Annotating Genomic Ranges. *PLOS Comput. Biol.* **9**, e1003118 (2013).

45. Wickham, H. *et al.* Welcome to the Tidyverse. *J. Open Source Softw.* **4**, 1686 (2019).

46. Wood, D. E., Lu, J. & Langmead, B. Improved metagenomic analysis with Kraken 2. *Genome Biol.* **20**, 257 (2019).

47. Li, H. Minimap2: pairwise alignment for nucleotide sequences. *Bioinformatics* **34**, 3094–3100 (2018).

48. Li, H. *et al.* The Sequence Alignment/Map format and SAMtools. *Bioinformatics* **25**, 2078–2079 (2009).

49. Martin, M. Cutadapt removes adapter sequences from high-throughput sequencing reads. *EMBnet.journal* **17**, 10–12 (2011).

50. Zheng, Z. *et al.* Symphonizing pileup and full-alignment for deep learning-based long-read variant calling. *Nat. Comput. Sci.* **2**, 797–803 (2022).

51. Quinlan, A. R. & Hall, I. M. BEDTools: a flexible suite of utilities for comparing genomic features. *Bioinformatics* **26**, 841–842 (2010).

52. Ewels, P., Magnusson, M., Lundin, S. & Käller, M. MultiQC: summarize analysis results for multiple tools and samples in a single report. *Bioinformatics* **32**, 3047–3048 (2016).

53. Wickham, H. *Ggplot2: Elegant Graphics for Data Analysis*. (Springer International Publishing, 2016). doi:10.1007/978-3-319-24277-4.

54. R Core Team. R: A Language and Environment for Statistical Computing. R Foundation for Statistical Computing (2014).

55. Briatte, F. ggnetwork: Geometries to Plot Networks with 'ggplot2'. (2021).

56. Csárdi, G. *et al.* igraph for R: R interface of the igraph library for graph theory and network analysis. (2023) doi:10.5281/zenodo.8240644.

Supplementary Figure 1. Population structure and characteristics of initial *Treponema* dataset used for Phylo-Plex design. A – Maximum Likelihood phylogeny of 607 *Treponema pallidum* genomes, with coloured tracks showing Subspecies, Lineage (within subspecies pallidum), and Sublineage (across all subspecies). B - Treemap plot showing distribution of genomes by *T. pallidum* subspecies: TPA – subspecies *pallidum*, TPE – subspecies *pertenue*, TEN – subspecies *endemicum*. C - Treemap plot showing distribution of genomes by T. pallidum subspecies (clustered as samples sharing a common ancestral node ≤10 SNPs. D - Treemap plot showing distribution of genomes by country.

Supplementary Figure 2. Identifying discriminatory SNPs for a single lineage.
A – Population fixation analysis (F_{ST}) of variable sites. Sites in red discriminate *T. pallidum* Nichols Lineage from all other lineages at $F_{ST} \geq 0.9$. B – Maximum likelihood whole genome phylogeny showing allelic identity at each discriminatory site identified in A. Colours indicate allele detected (pale grey indicates 'N', where data was missing – common in metagenomic data).

Supplementary Figure 3. Identifying discriminatory SNPs for 40 sublineages.
Population fixation analysis (F_{ST}) of variable sites for each sublineage - plots show only sites with $F_{ST} \geq 0.9$.

Supplementary Figure 4. Discriminatory site support for each sublineage.
Plot shows number of discriminatory sites specifically supporting each lineage and sublineage when considering (i) all discriminatory sites identified in the genome dataset, (ii) sites included in 74 regions selected by the Phylo-Plex selection algorithm, (iii) sites remaining after full optimization of the 59-amplicon multiplex PCR. The final PCR used for evaluation removed 15 amplicons and therefore removed direct support for 8 sublineages ('*'), but future iterations would modify the primer designs and balance to reinclude these.

Supplementary Figure 5. Genomic distance between individual sites is reduced when considered as a total population.
Genetic distance between adjacent discriminatory SNPs according to sublineage and as a total population. Blue line highlights 300 bp.

Supplementary Figure 6. Changing distance used to link SNPs as clusters impacts cluster count, SNPs per amplicon and minimum amplicon size.
The selection of an appropriate genomic distance for positional clustering can be tuned and impacts the number of SNPs that merge into clusters. However, increasing cluster distance

between individual SNPs can also substantially impact the total length of SNP networks, resulting in candidate amplicons too long to reasonably amplify in multiplex PCR. A – Number of positional clusters produced with different genomic distance between sites. B – Number of SNPs present in each cluster (candidate amplicon) produced with different genomic distance between sites. C – Genomic distance between furthest SNPs in cluster (i.e. minimum length of candidate amplicon) produced with different genomic distance between sites.

Supplementary Figure 7. Hierarchical selection algorithm for maximising discriminatory power whilst minimising total number of amplicons.

Each candidate region is evaluated based on the sublineages the SNPs within it support, and regions are added until support for a sublineage meets a minimum threshold (3 SNPs), after which, support for that sublineage is no longer considered.

Supplementary Figure 8. Sequencing performance of 72 South African clinical syphilis samples.

Points show mean coverage for 74 amplicons from each of 72 samples, ordered by input Treponema qPCR Ct. Blue line indicates 25X coverage threshold. Red points indicate 15 amplicons which consistently performed poorly.

Supplementary Figure 9. Sequencing performance of 74 multiplex amplicons in clinical syphilis samples.

Points show mean coverage for 74 amplicons from each of 72 South African clinical syphilis samples compared to input Treponema qPCR Ct. Blue line indicates 25X coverage threshold. Red points indicate 15 amplicons in the bottom 5% for performance.

Supplementary Figure 10. Quantitative comparison between WGS derived phylogeny and Amplicon derived phylogeny demonstrates high concordance.

A – Collapsed WGS phylogeny (one tip per sublineage), B – Tree concordance between collapsed WGS tree and (i) full WGS tree, (ii) Amplicon derived tree (simulated), (iii) 100 bootstraps derived from full WGS tree, (iv) 100 tip-randomised full WGS trees.

Supplementary Figure 11. *In silico* sublineage concordance between WGS and amplicons.

A – Collapsed WGS phylogeny (one tip per sublineage), against Amplicon profiles (identical sequences). Each column represents a cluster of identical amplicon profiles, coloured by the whole genome sublineage. Amplicon profiles which include multiple sublineages (indicated

by arrows) are not fully resolved. Some sublineages consist of multiple amplicon profiles, reflecting expected SNP diversity in the amplicons. B – Distribution of samples within the amplicon profiles according to sublineage. Bars are coloured by sublineage proportion, and numbers indicate the genome count in the analysis.

Supplementary Figure 12. *In silico* reconstruction of UK syphilis population structure using genomes and amplicons.

A – Minimum spanning tree of UK syphilis genomes coloured by sublineages (Beale 2023). Branch lengths indicate SNPs, and dotted lines indicate truncated branches ≥20 SNPs. B – Minimum spanning tree of UK syphilis dataset simulated using final 59-amplicon TP-Phylo-Plex scheme.

Supplementary Figure 13. Amplicon recovery for 17 samples at Zimbabwe field site.

Points show mean coverage for 59 amplicons from each of 14 samples collected, processed and sequenced in Zimbabwe, ordered by input Treponema qPCR Ct. Blue line indicates 25X coverage threshold. Includes technical replicates (mz476a/b, mz446a/b/c).

Supplementary Figure 14. Phylo-Plex can detect *de novo* mutations and novel sublineages but is insensitive to minor changes.

In silico mutations in whole *T. pallidum* genomes contained within TP-Phylo-Plex amplicons (250 simulations). With 0.001% genomic sites mutated (11 SNPs – similar to discriminatory level within most *T. pallidum* sub-lineages), only 5.2% of replicates had ≥2 SNPs occurring within Phy-cons. However, at 0.005% genome sites mutated (56 SNPs), this rose to 45.6% of replicates, and at 0.01% genomic sites (113 SNPs), it rose to 87.6% of replicates. Blue line indicates 2 SNPs (minimum SNPs needed to theoretically detect a sublineage as different in amplicon data).

Supplementary Figure 15. Workflow of NextFlow pipeline for automated processing of Phylo-Plex amplicon sequence data.

Complete workflow for processing raw ONT sequence files (POD5/Fast5), including basecalling, quality assessment, trimming and filtering, mapping, coverage assessment, variant calling and pseudosequence generation.

Supplementary Table 1. Metadata and list of genomes used for designing the TP-Phylo-Plex scheme.

Supplementary Table 2. Primers designed for TP-Phylo-Plex scheme.

Supplementary Table 3. Description of sequences and metadata for validation samples from South Africa.

Supplementary Table 4. Description of sequences and metadata for field work samples from Zimbabwe.

1

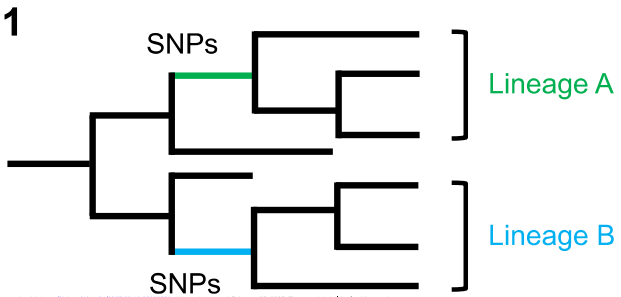

Identify lineage discriminatory SNPs

2

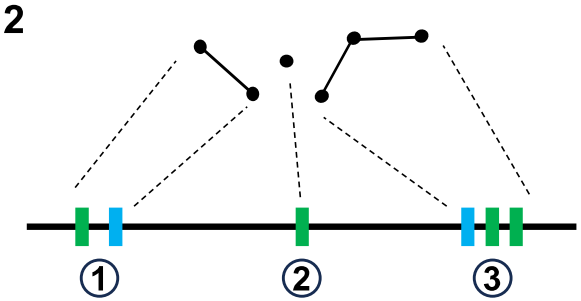

Network inference of positional clustering

3

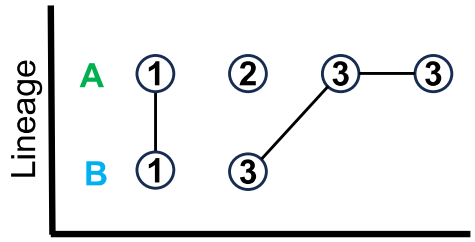

Hierarchical selection algorithm to maximise allelic discrimination and minimise regions

4

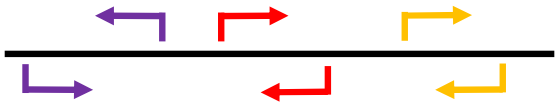

Automated multiplex primer design

5

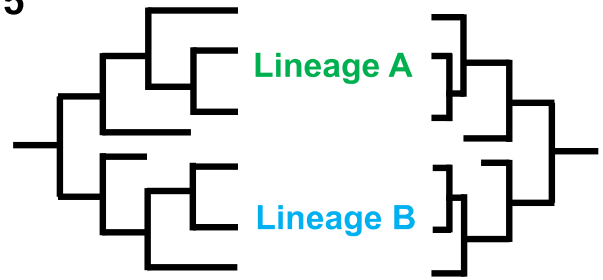

In silico validation

6

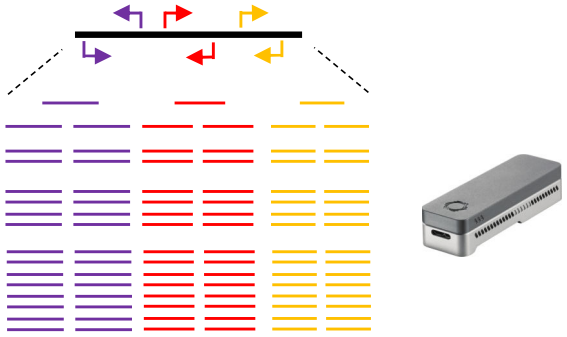

Laboratory PCR and sequencing

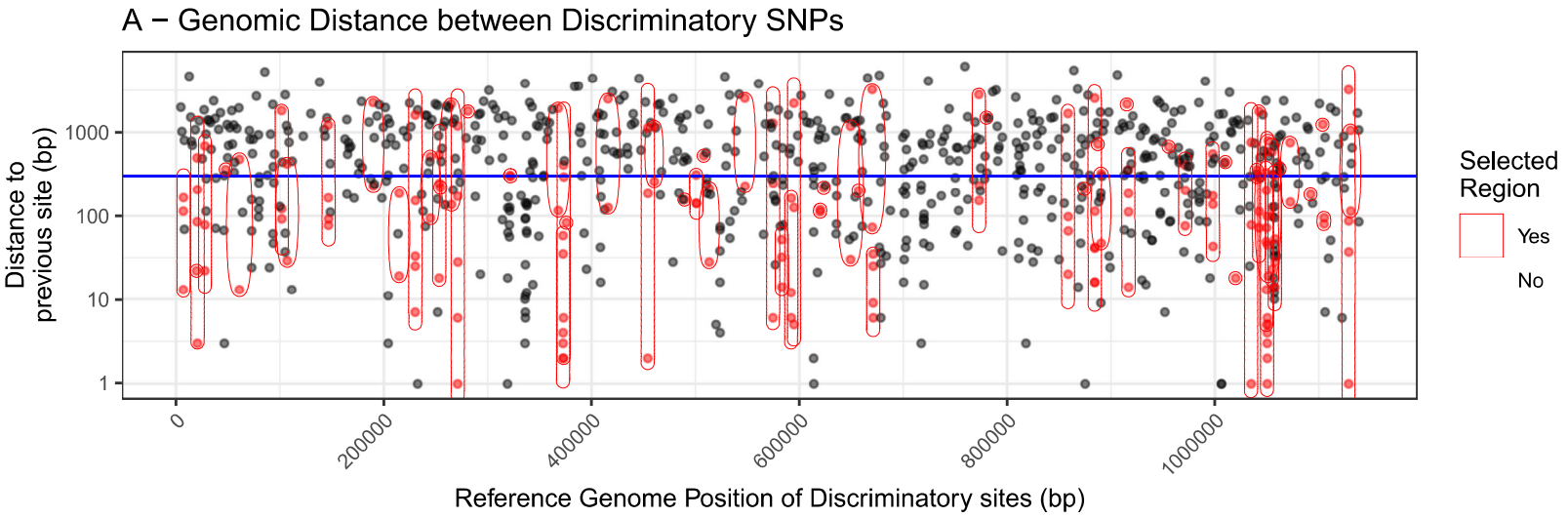

B − Network of Discriminatory SNPs <=300bp apart

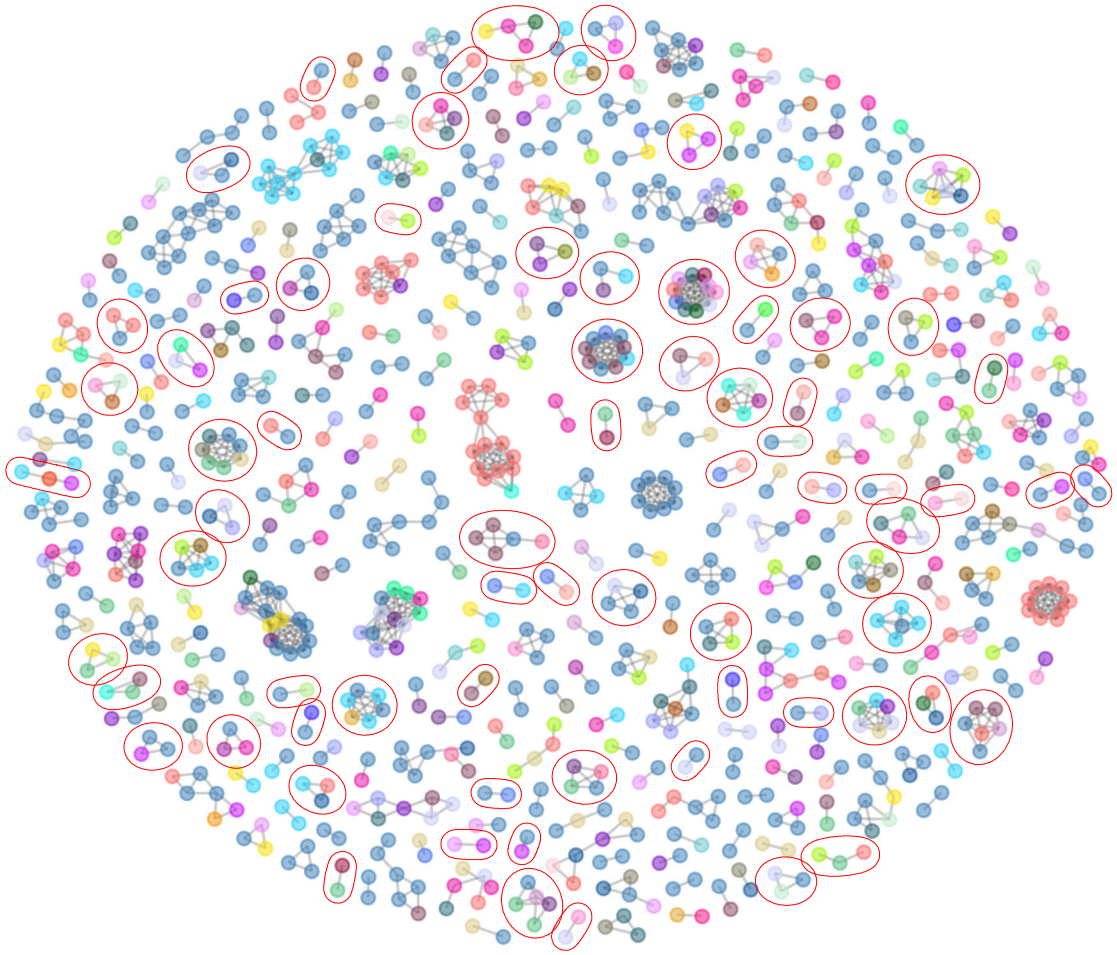

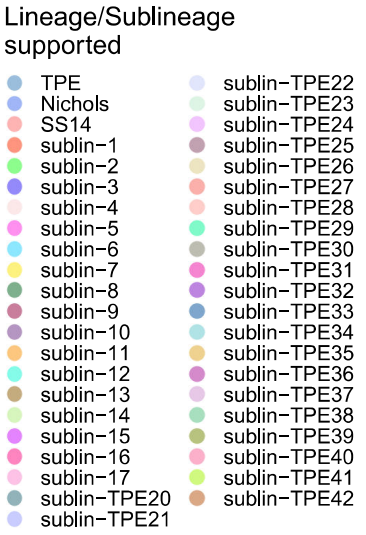

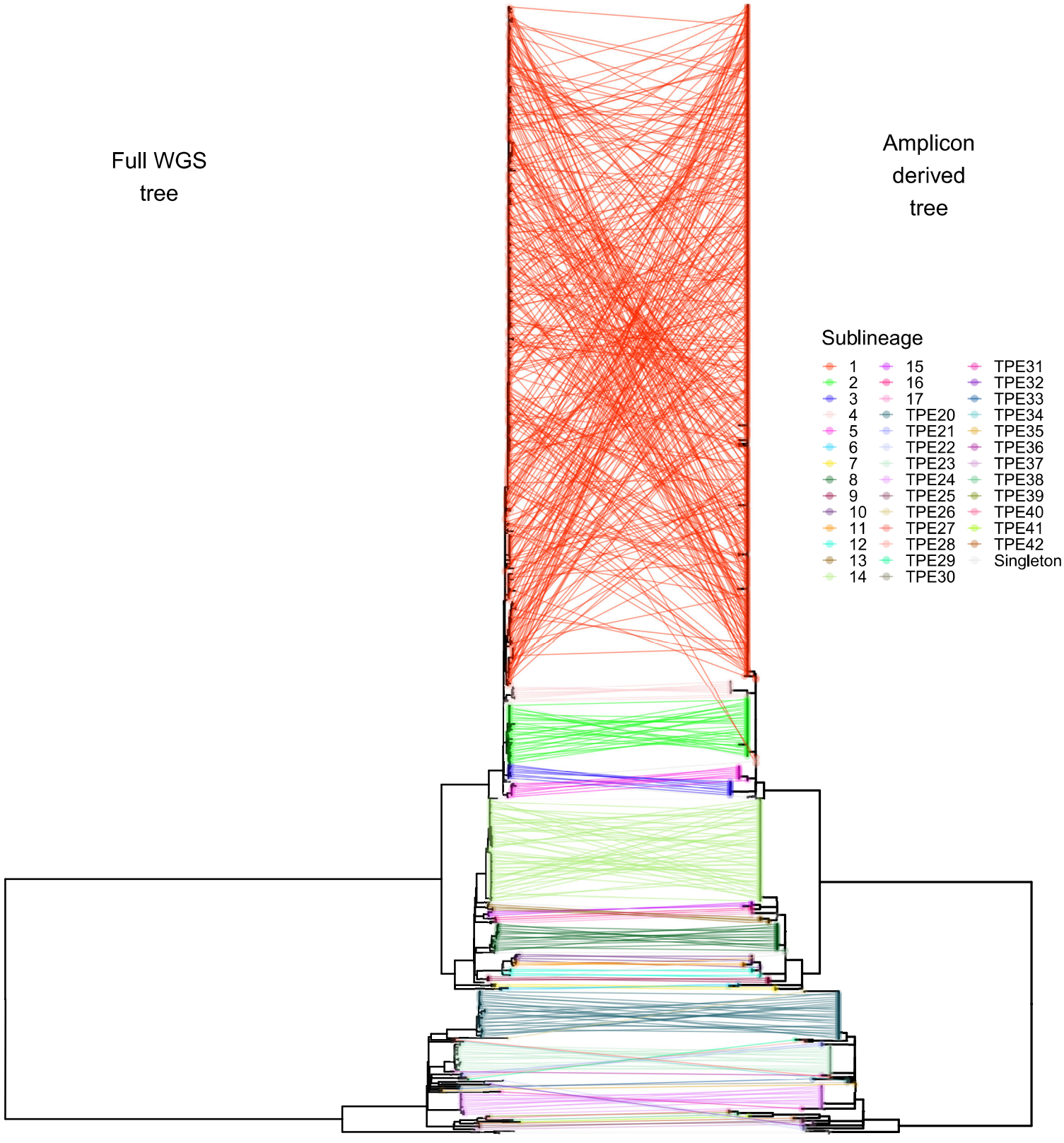
Full WGS tree
Amplicon derived tree
Sublineage
1
2
3
4
5
6
7
8
9
10
11
12
13
14
15
16
17
TPE20
TPE21
TPE22
TPE23
TPE24
TPE25
TPE26
TPE27
TPE28
TPE29
TPE30
TPE31
TPE32
TPE33
TPE34
TPE35
TPE36
TPE37
TPE38
TPE39
TPE40
TPE41
TPE42
Singleton

~2 hrs

DNA Extraction

~2 hrs

Diagnostics

~8 hrs

Amplicons & Library Preparation

~10-12 hrs

Sequencing

~30 mins

Bioinformatics & Results

gDNA

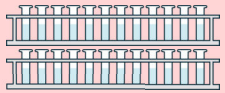

n=24

Multiplex PCR

Confirm Amplicons

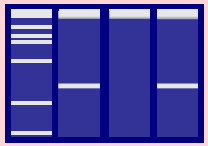

Ligate

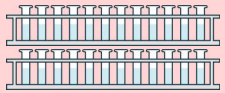

Indices

Pool

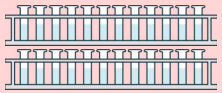

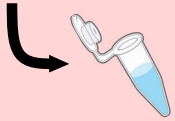

Cleanup & add adaptors

Sequence

MinION Flongle

A − Whole Genome Phylogeny

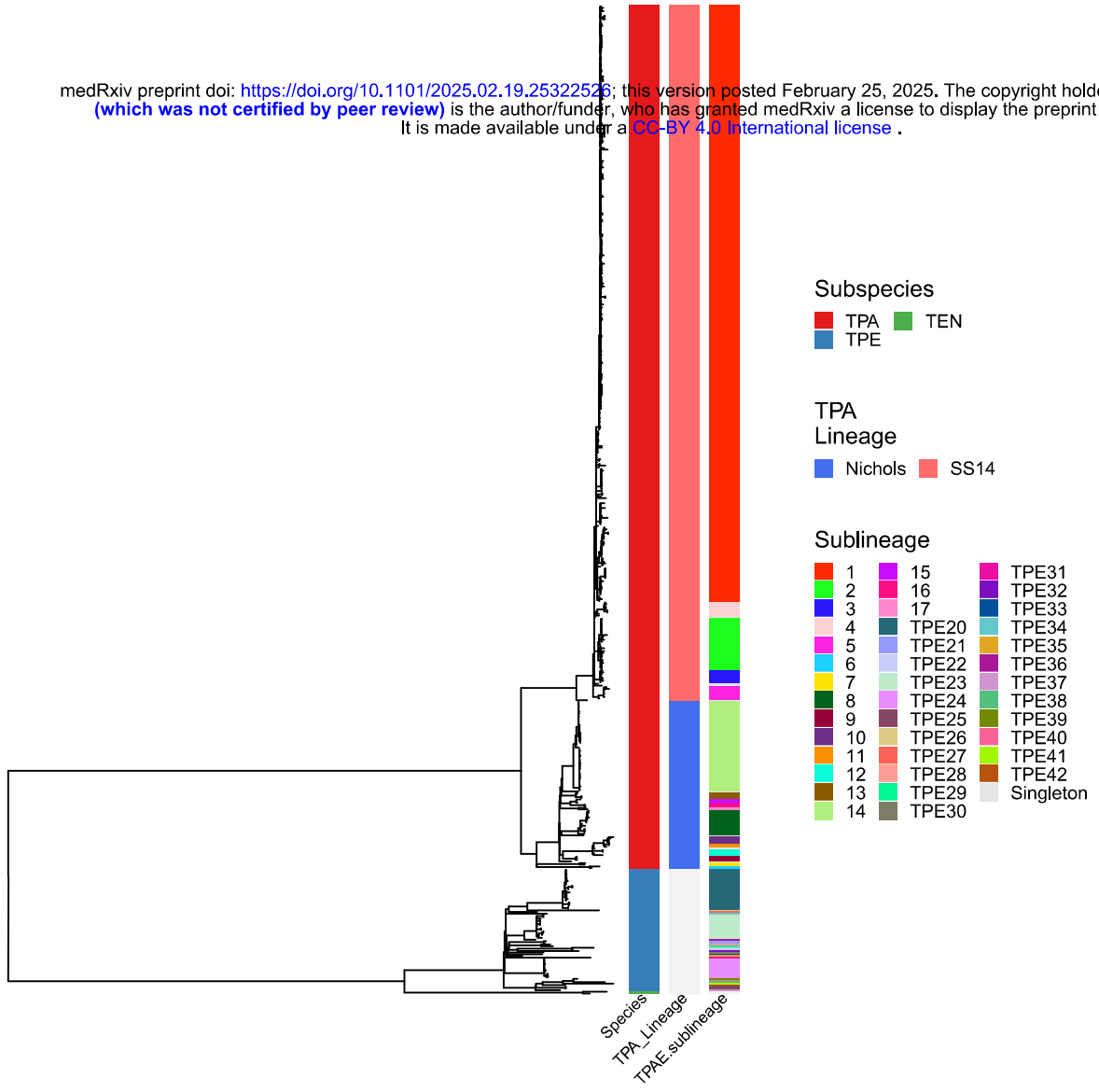

B − Subspecies distributions

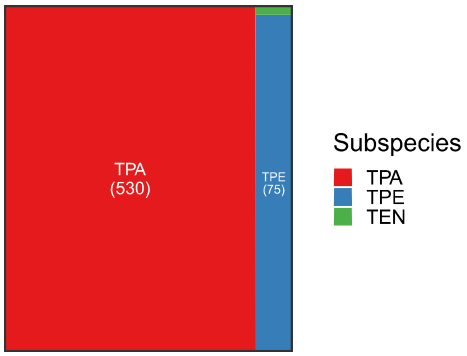

C − Sublineage distributions

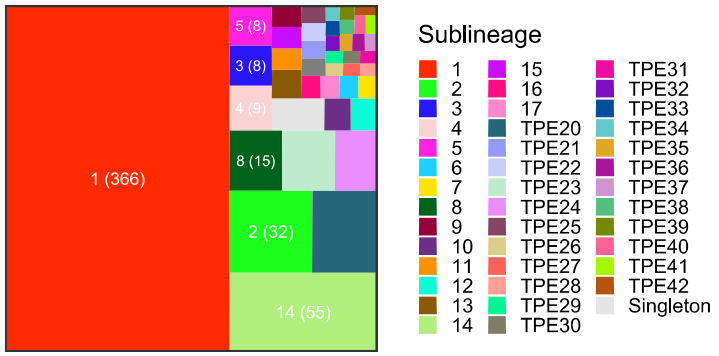

D − Geographical distributions

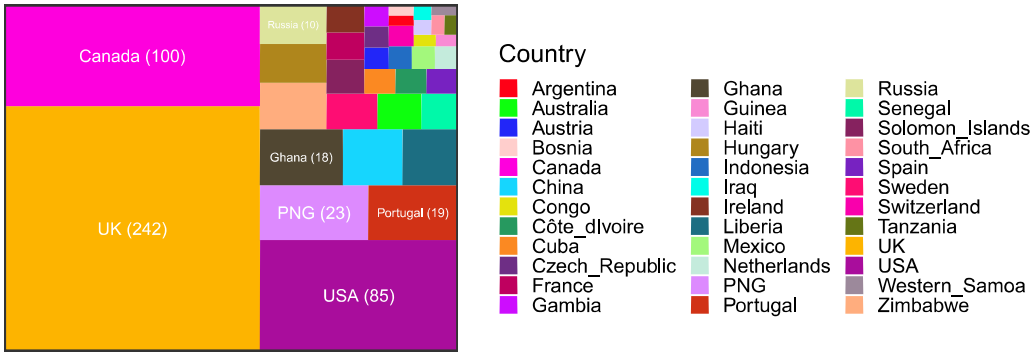

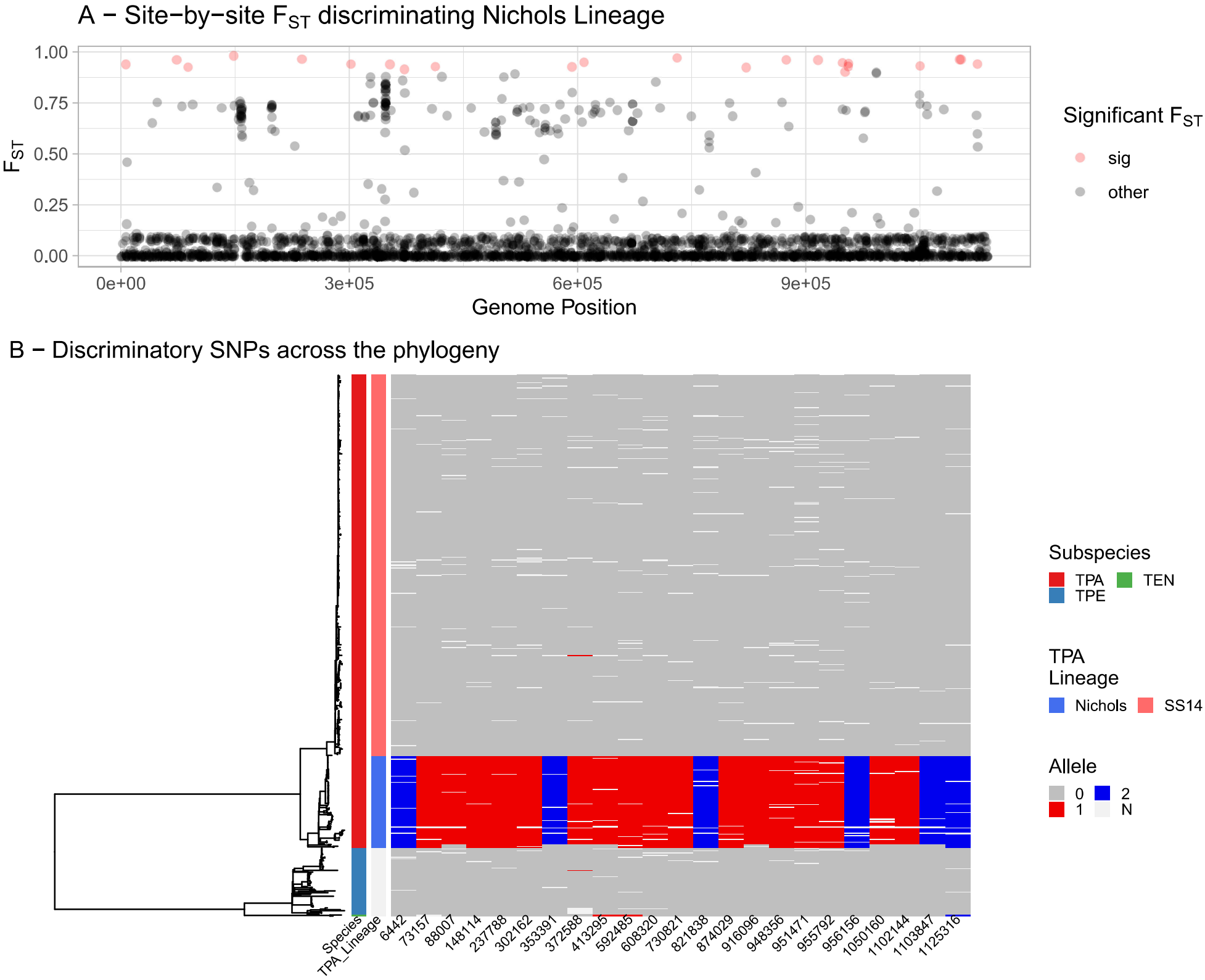
A − Site−by−site F_{ST} discriminating Nichols Lineage
1.00
0.75
0.50
0.25
0.00
F_{ST}
0e+00
3e+05
6e+05
9e+05
Genome Position
Significant F_{ST}
sig
other
B − Discriminatory SNPs across the phylogeny
Species
TPA_Lineage
6442
73157
88007
148114
237788
302162
353391
372588
413295
592485
608320
730821
821838
874029
916096
948356
951471
955792
956156
1050160
1102144
1103847
1125316
Subspecies
TPA
TEN
TPE
TPA Lineage
Nichols
SS14
Allele
0
2
1
N

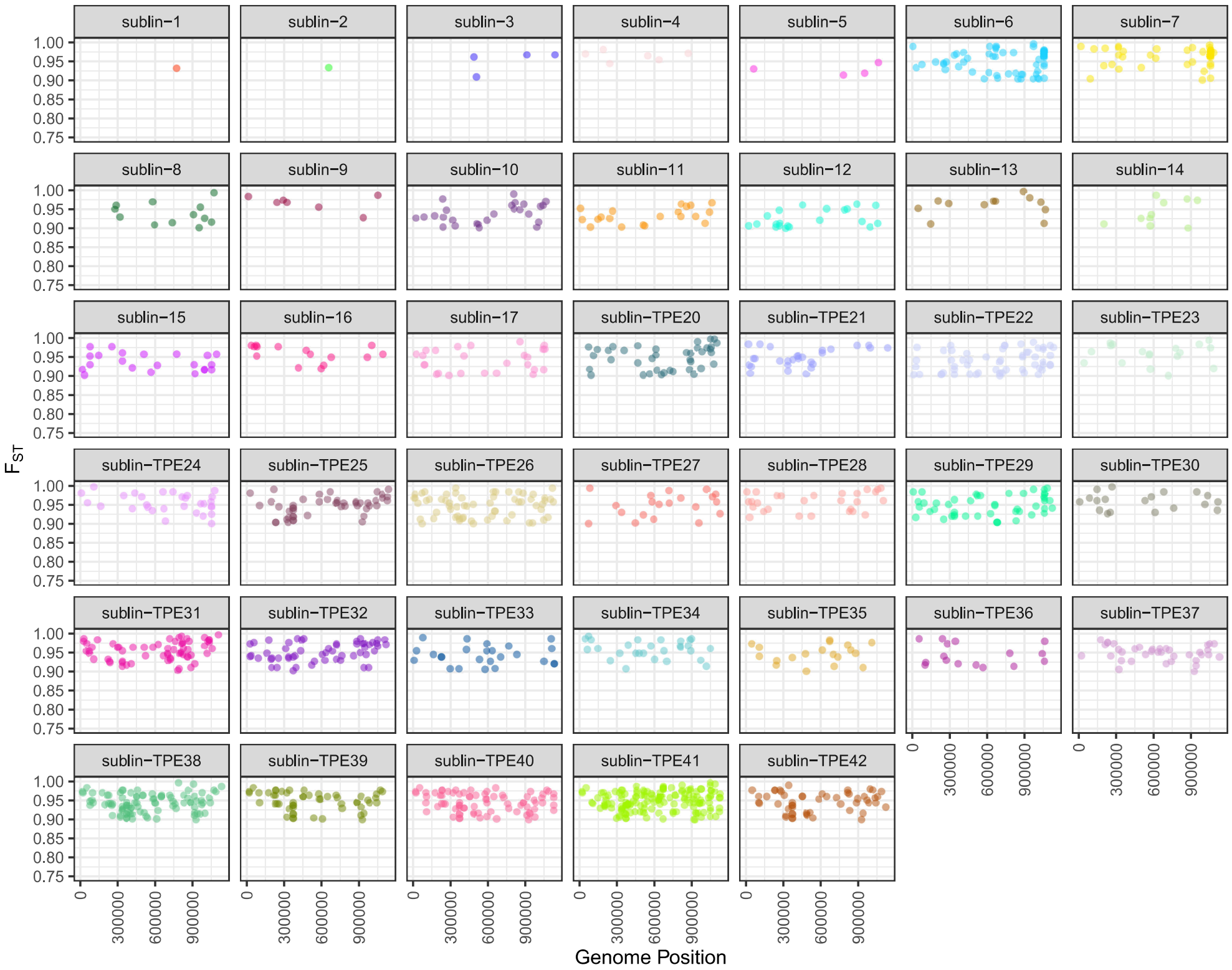
855 discriminating alleles across all 40 defined sublineages
sublin−1
sublin−2
sublin−3
sublin−4
sublin−5
sublin−6
sublin−7
sublin−8
sublin−9
sublin−10
sublin−11
sublin−12
sublin−13
sublin−14
sublin−15
sublin−16
sublin−17
sublin−TPE20
sublin−TPE21
sublin−TPE22
sublin−TPE23
sublin−TPE24
sublin−TPE25
sublin−TPE26
sublin−TPE27
sublin−TPE28
sublin−TPE29
sublin−TPE30
sublin−TPE31
sublin−TPE32
sublin−TPE33
sublin−TPE34
sublin−TPE35
sublin−TPE36
sublin−TPE37
sublin−TPE38
sublin−TPE39
sublin−TPE40
sublin−TPE41
sublin−TPE42
1.00
0.95
0.90
0.85
0.80
0.75
F_{ST}
0
300000
600000
900000
Genome Position

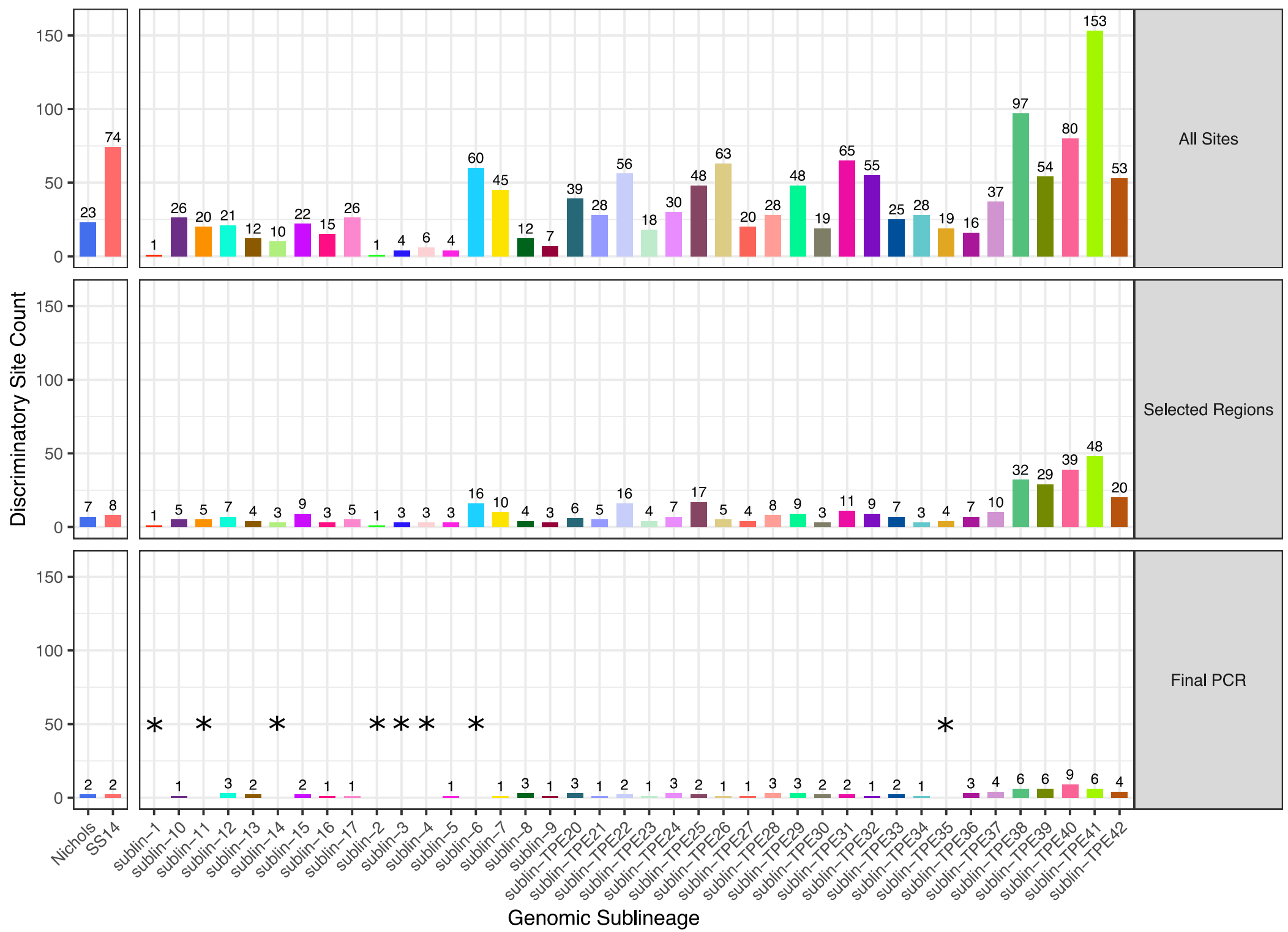
All Sites
Selected Regions
Final PCR
Discriminatory Site Count
Genomic Sublineage
Nichols
SS14
sublin–1
sublin–10
sublin–11
sublin–12
sublin–13
sublin–14
sublin–15
sublin–16
sublin–17
sublin–2
sublin–3
sublin–4
sublin–5
sublin–6
sublin–7
sublin–8
sublin–9
sublin–TPE20
sublin–TPE21
sublin–TPE22
sublin–TPE23
sublin–TPE24
sublin–TPE25
sublin–TPE26
sublin–TPE27
sublin–TPE28
sublin–TPE29
sublin–TPE30
sublin–TPE31
sublin–TPE32
sublin–TPE33
sublin–TPE34
sublin–TPE35
sublin–TPE36
sublin–TPE37
sublin–TPE38
sublin–TPE39
sublin–TPE40
sublin–TPE41
sublin–TPE42

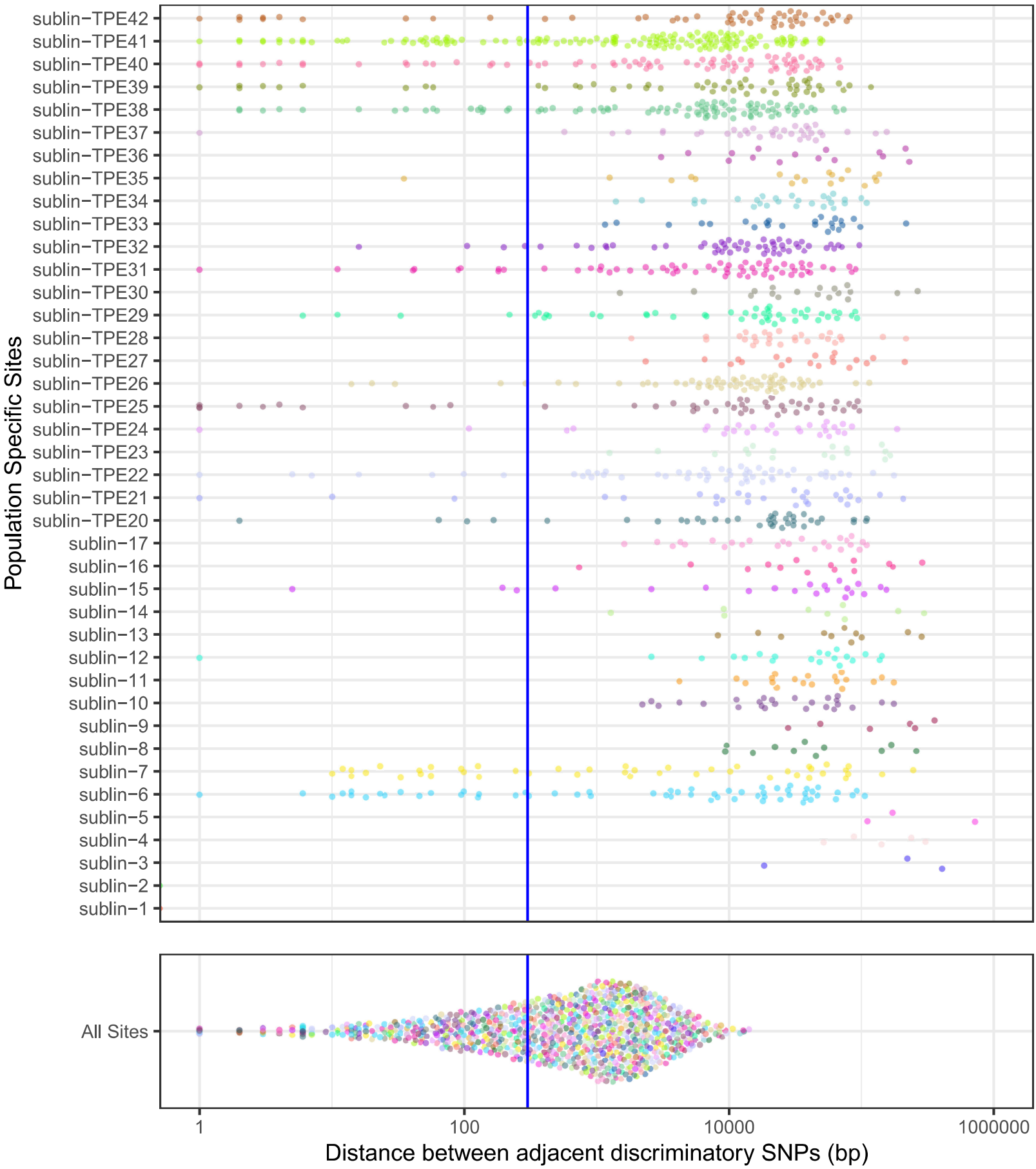
Population Specific Sites
sublin−TPE42
sublin−TPE41
sublin−TPE40
sublin−TPE39
sublin−TPE38
sublin−TPE37
sublin−TPE36
sublin−TPE35
sublin−TPE34
sublin−TPE33
sublin−TPE32
sublin−TPE31
sublin−TPE30
sublin−TPE29
sublin−TPE28
sublin−TPE27
sublin−TPE26
sublin−TPE25
sublin−TPE24
sublin−TPE23
sublin−TPE22
sublin−TPE21
sublin−TPE20
sublin−17
sublin−16
sublin−15
sublin−14
sublin−13
sublin−12
sublin−11
sublin−10
sublin−9
sublin−8
sublin−7
sublin−6
sublin−5
sublin−4
sublin−3
sublin−2
sublin−1
All Sites
1
100
10000
1000000
Distance between adjacent discriminatory SNPs (bp)

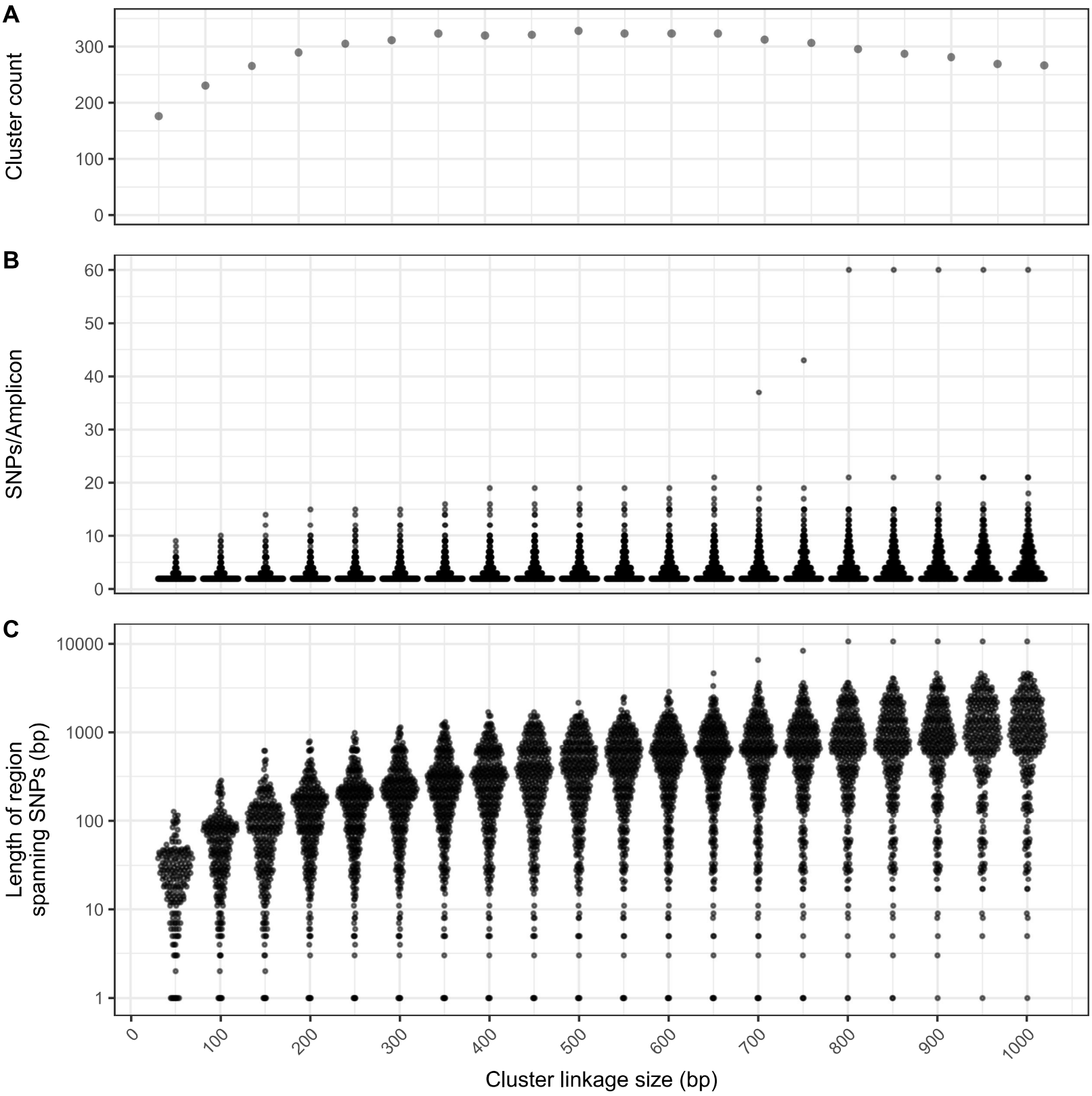
A
Cluster count
300
200
100
0
B
SNPs/Amplicon
60
50
40
30
20
10
0
C
Length of region spanning SNPs (bp)
10000
1000
100
10
1
0
100
200
300
400
500
600
700
800
900
1000
Cluster linkage size (bp)

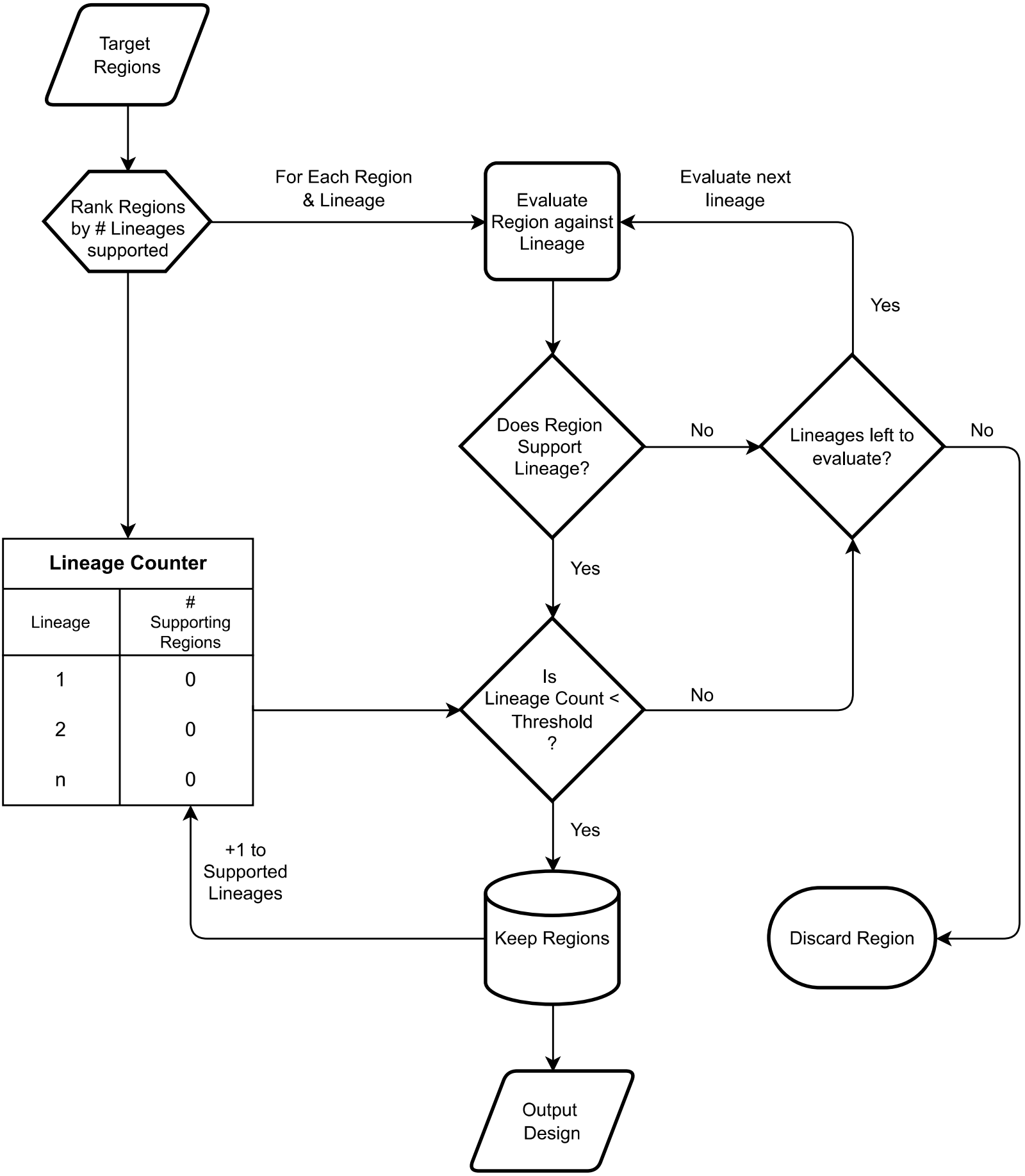
Target Regions
Rank Regions by # Lineages supported
For Each Region & Lineage
Evaluate Region against Lineage
Evaluate next lineage
Yes
Does Region Support Lineage?
No
Lineages left to evaluate?
No
Yes
Lineage Counter
Lineage
Supporting Regions
1
0
2
0
n
0
Is Lineage Count < Threshold ?
No
Yes
+1 to Supported Lineages
Keep Regions
Discard Region
Output Design

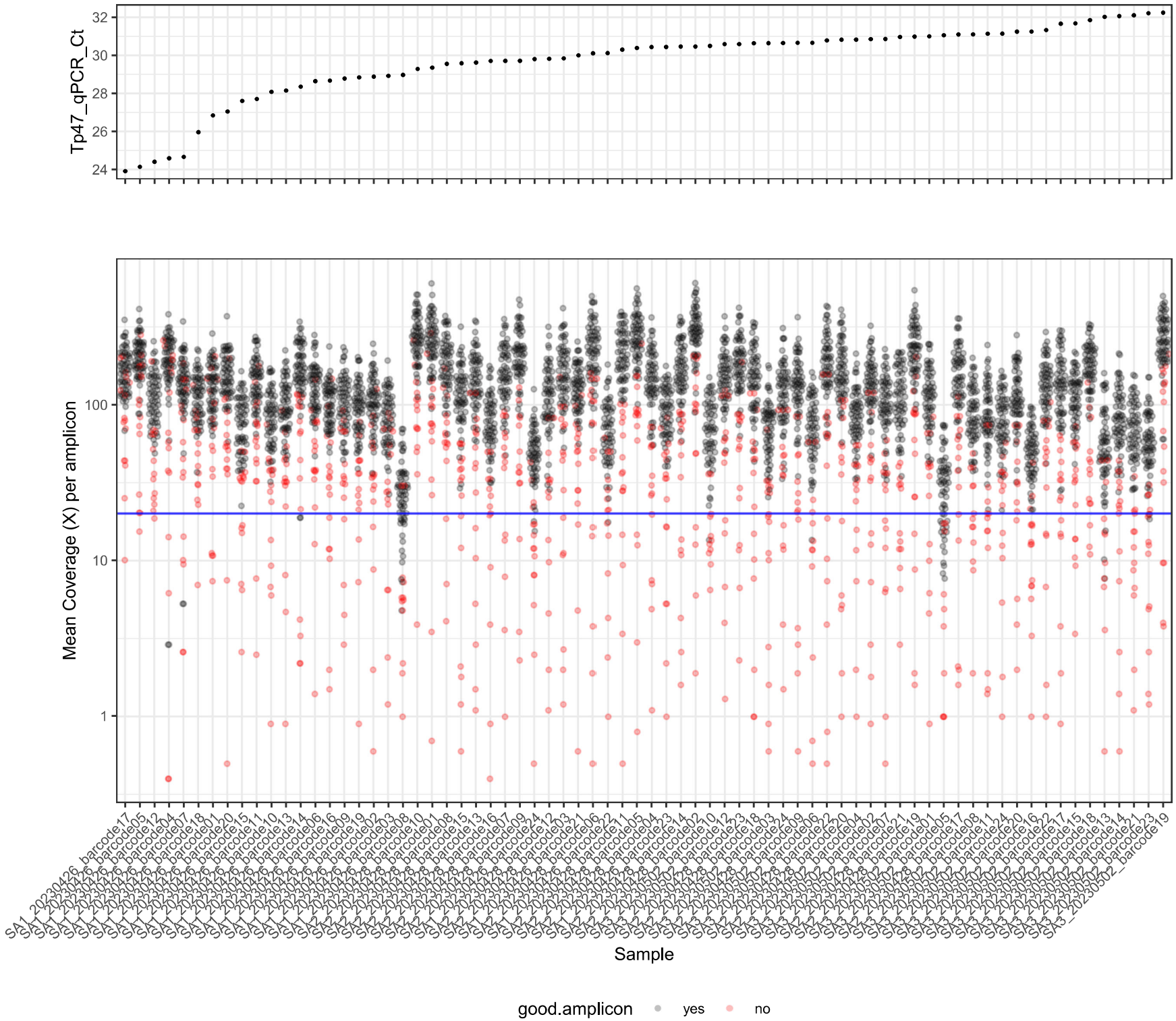
Tp47_qPCR_Ct
32
30
28
26
24
Mean Coverage (X) per amplicon
100
10
1
Sample
good.amplicon
yes
no

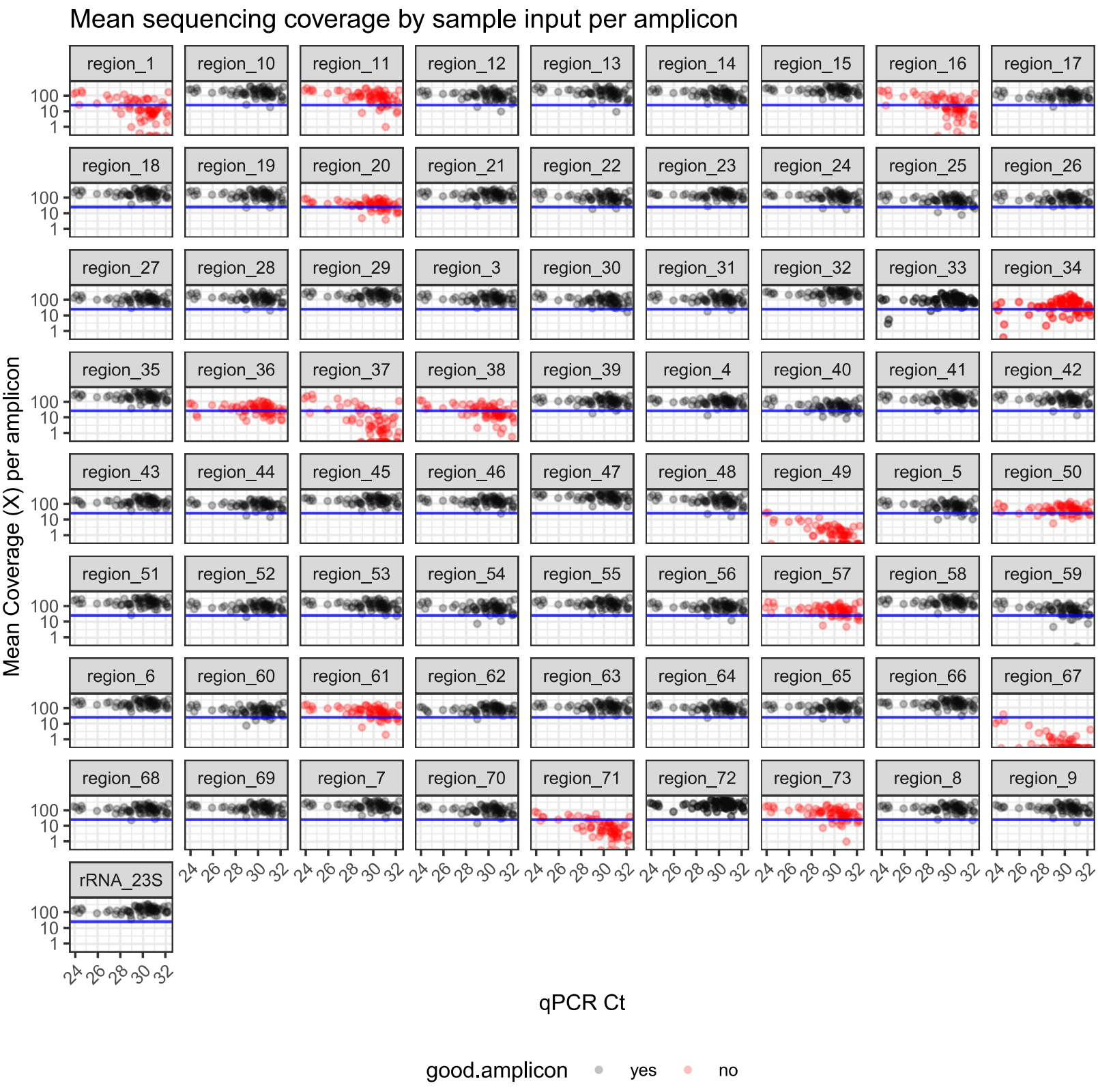
Mean sequencing coverage by sample input per amplicon
region_1
region_10
region_11
region_12
region_13
region_14
region_15
region_16
region_17
region_18
region_19
region_20
region_21
region_22
region_23
region_24
region_25
region_26
region_27
region_28
region_29
region_3
region_30
region_31
region_32
region_33
region_34
region_35
region_36
region_37
region_38
region_39
region_4
region_40
region_41
region_42
region_43
region_44
region_45
region_46
region_47
region_48
region_49
region_5
region_50
region_51
region_52
region_53
region_54
region_55
region_56
region_57
region_58
region_59
region_6
region_60
region_61
region_62
region_63
region_64
region_65
region_66
region_67
region_68
region_69
region_7
region_70
region_71
region_72
region_73
region_8
region_9
rRNA_23S
100
10
1
24
26
28
30
32
Mean Coverage (X) per amplicon
qPCR Ct
good.amplicon
yes
no

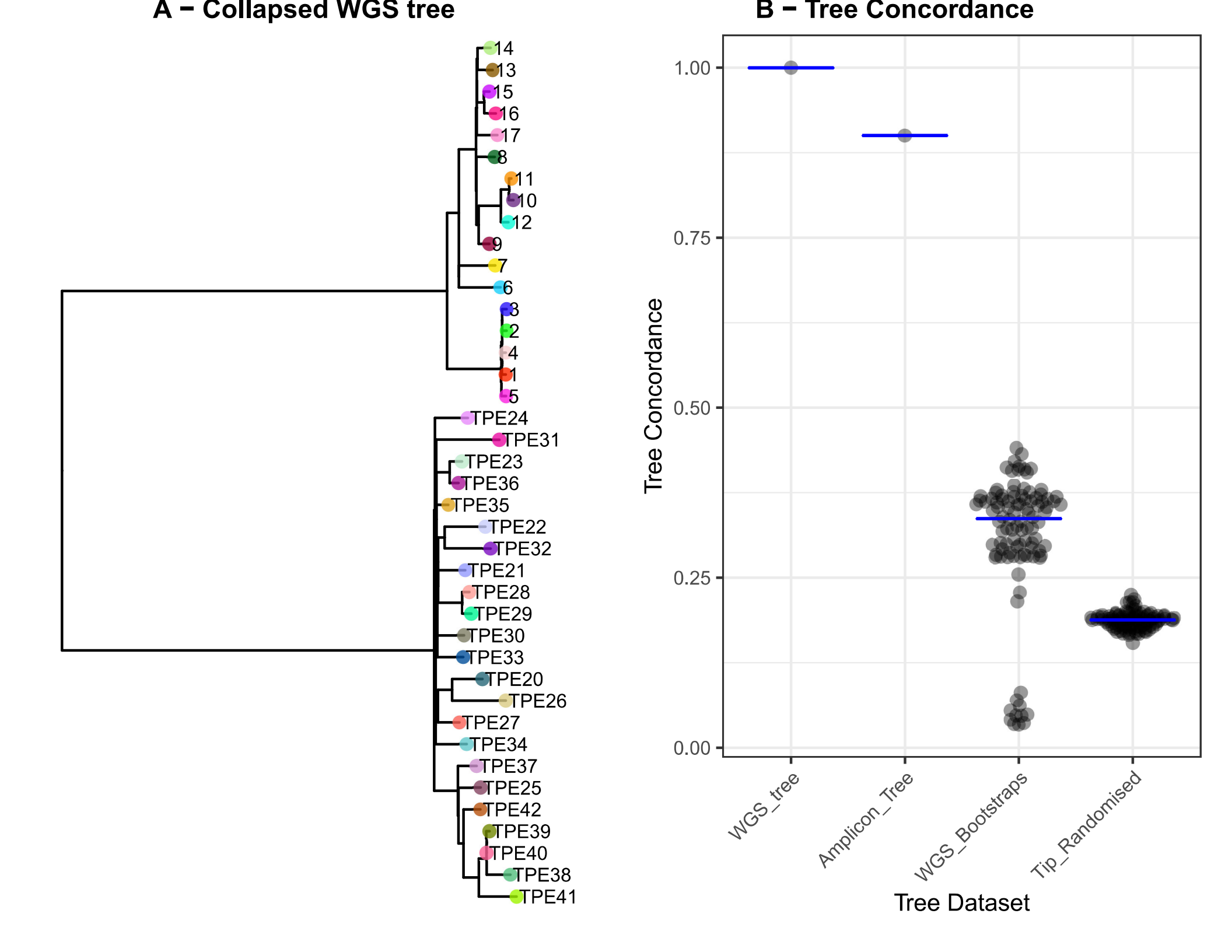
A – Collapsed WGS tree
14
13
15
16
17
8
11
10
12
9
7
6
3
2
4
1
5
TPE24
TPE31
TPE23
TPE36
TPE35
TPE22
TPE32
TPE21
TPE28
TPE29
TPE30
TPE33
TPE20
TPE26
TPE27
TPE34
TPE37
TPE25
TPE42
TPE39
TPE40
TPE38
TPE41
B – Tree Concordance
Tree Concordance
1.00
0.75
0.50
0.25
0.00
WGS_tree
Amplicon_Tree
WGS_Bootstraps
Tip_Randomised
Tree Dataset

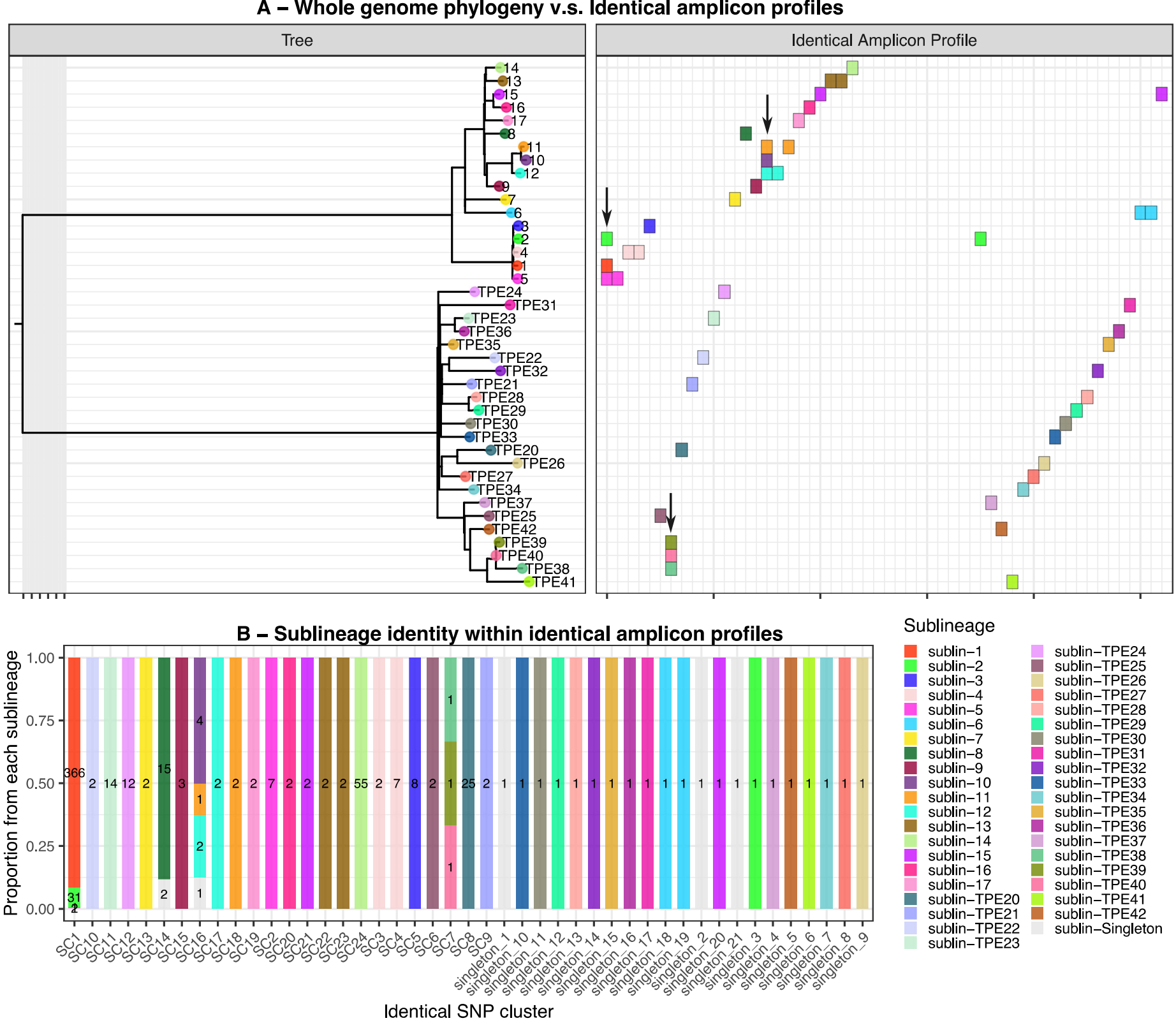
A – Whole genome phylogeny v.s. Identical amplicon profiles
Tree
Identical Amplicon Profile
14
13
15
16
17
8
11
10
12
9
7
6
3
2
4
1
5
TPE24
TPE31
TPE23
TPE36
TPE35
TPE22
TPE32
TPE21
TPE28
TPE29
TPE30
TPE33
TPE20
TPE26
TPE27
TPE34
TPE37
TPE25
TPE42
TPE39
TPE40
TPE38
TPE41
B – Sublineage identity within identical amplicon profiles
Proportion from each sublineage
1.00
0.75
0.50
0.25
0.00
Identical SNP cluster
Sublineage
sublin–1
sublin–2
sublin–3
sublin–4
sublin–5
sublin–6
sublin–7
sublin–8
sublin–9
sublin–10
sublin–11
sublin–12
sublin–13
sublin–14
sublin–15
sublin–16
sublin–17
sublin–TPE20
sublin–TPE21
sublin–TPE22
sublin–TPE23
sublin–TPE24
sublin–TPE25
sublin–TPE26
sublin–TPE27
sublin–TPE28
sublin–TPE29
sublin–TPE30
sublin–TPE31
sublin–TPE32
sublin–TPE33
sublin–TPE34
sublin–TPE35
sublin–TPE36
sublin–TPE37
sublin–TPE38
sublin–TPE39
sublin–TPE40
sublin–TPE41
sublin–TPE42
sublin–Singleton

A − UK WGS network

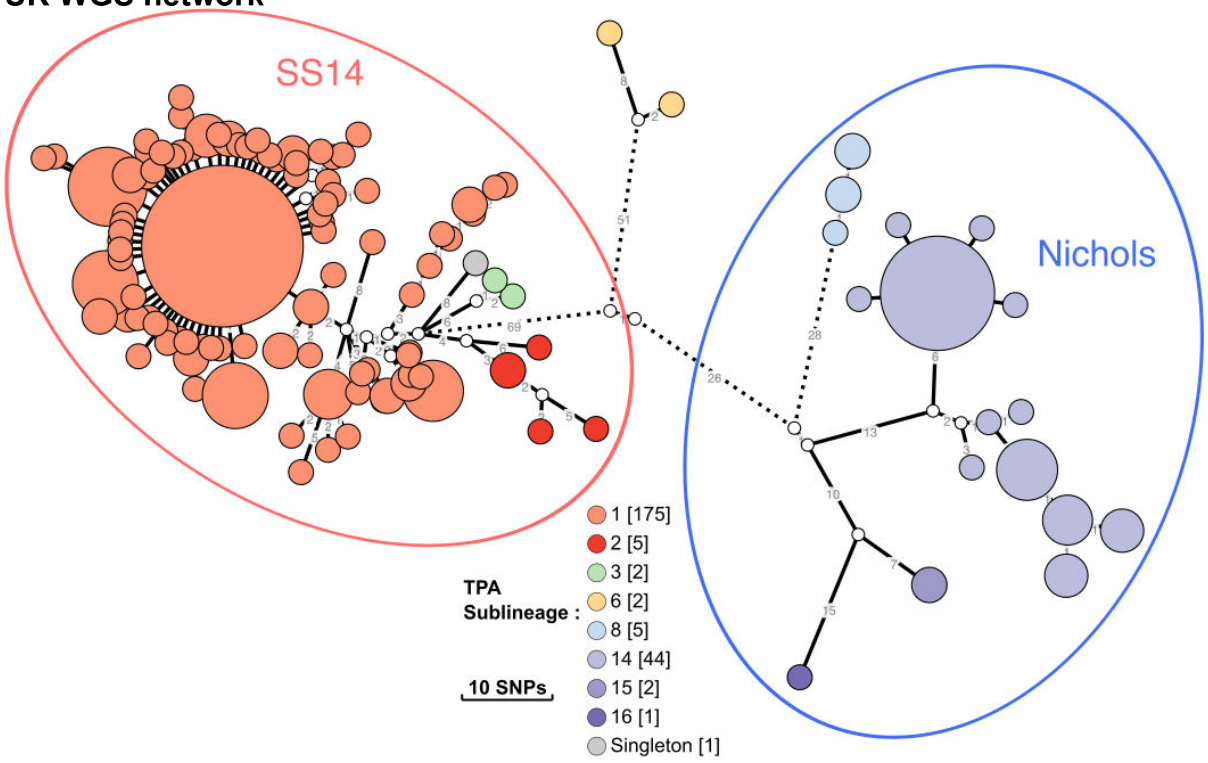

B − UK AmpliSeq network (inferred)

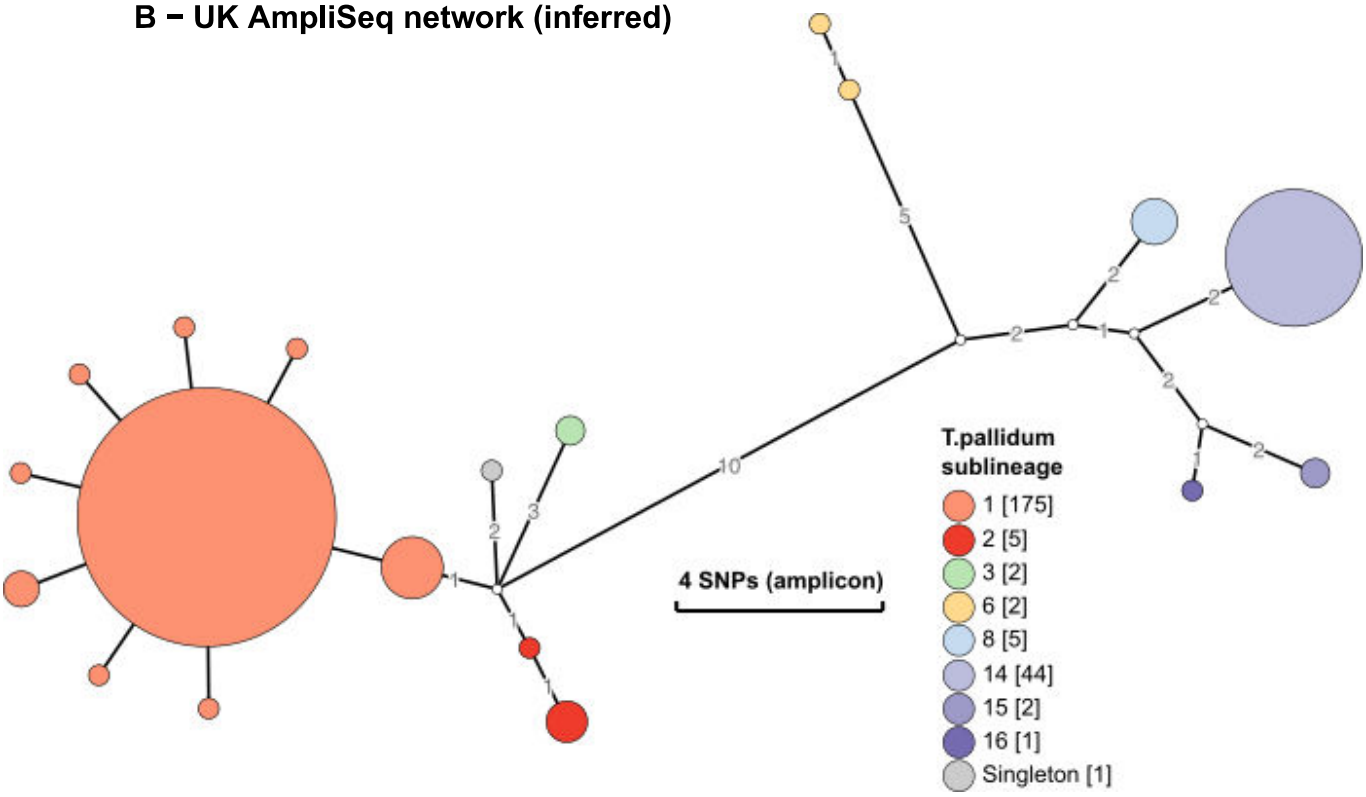

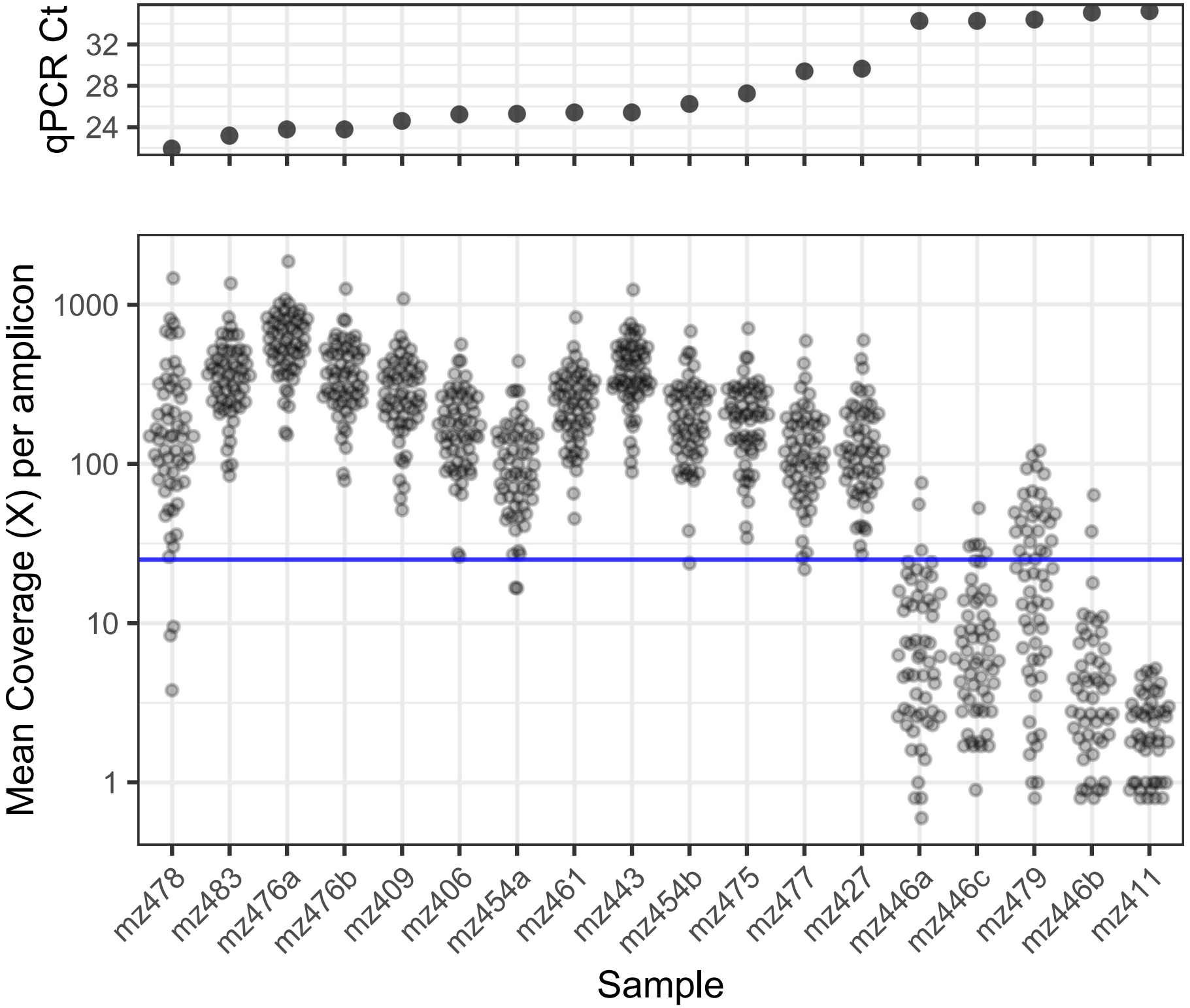
qPCR Ct
32
28
24
Mean Coverage (X) per amplicon
1000
100
10
1
mz478
mz483
mz476a
mz476b
mz409
mz406
mz454a
mz461
mz443
mz454b
mz475
mz477
mz427
mz446a
mz446c
mz479
mz446b
mz411
Sample

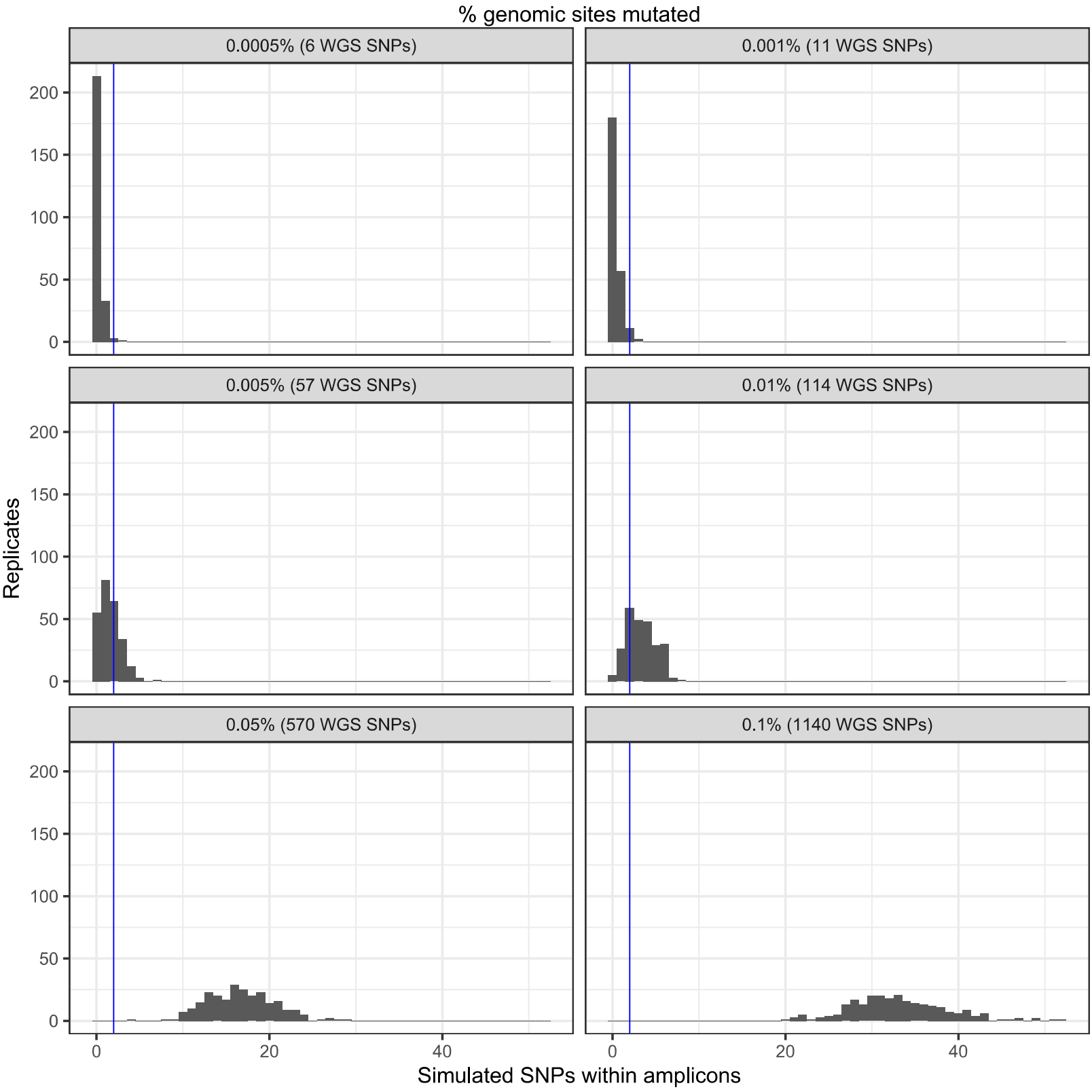
% genomic sites mutated
0.0005% (6 WGS SNPs)
0.001% (11 WGS SNPs)
0.005% (57 WGS SNPs)
0.01% (114 WGS SNPs)
0.05% (570 WGS SNPs)
0.1% (1140 WGS SNPs)
Replicates
Simulated SNPs within amplicons
0
50
100
150
200
0
20
40